UNIVERSIDAD CARLOS III DE MADRID

Bachelor thesis:

Computation of collision probability in Geostationary Orbit

Bachelor's Degree in Aerospace Engineering

Jesús Perales Díaz

Supervisor:
Manuel Sanjurjo Rivo

June 21, 2017

Contents

Chapter 1

Introduction

In the present work, the probability of collision between two orbiting bodies in a geostationary(or near geostationary) orbit will be addressed. Much has been written about the topic of computing the collision probability of satellites during the past decades. Certainly, the large volume of literature addressing this issue unveils the need that exists for ensuring the safety and integrity of the constantly growing population of satellites. The density of the "cloud" seems to increase without bound and the presence of debris puts into risk the operative satellites. Moreover, there is a specific ring, inside this "cloud" in which, due to its optimal conditions for communications or meteorological purposes, the increase of the mentioned "cloud density" is even larger: the Geostationary orbit.

The standard and widely accepted method for the estimation of the probability of collision is the well-known Monte Carlo simulation. Nevertheless, the large computational time required by this method may make it unfeasible to take real-time decision when there exist several collision risk situations at the same time. This is the reason why numerous approximated methods have been developed, aiming at reducing the computational time.

In LEO orbits, where satellites normally have not at all similar orbits, the satellite encounters(which are bounded by 3-sigma position error ellipsoids) occur at really large relative velocity and, as a result, the encounter time is very short. This fact is of paramount importance for the calculation of collision probability, since as the encounter is very brief, one simply needs to propagate the positions of the satellites to the point of closest approach and apply the existing methods[1][4][11]. These can be classified as linear relative motion methods, given that the relative velocity during the encounter can be considered to be linear. Now, if the orbits described by the satellites are similar, there is likelihood that their relative velocity is small. Thus, the encounter time will be large enough to prevent from assuming that the velocity does not change throughout the rendez-vous. This is the typical case observed in the region near the geostationary orbits, where all satellites try to be all as closed as possible to the mentioned orbit, which is unique. Several methods have been developed in order to solve this particular orbital rendez-vous in a relatively fast manner[2][9][3]. They must deal with changes in relative velocity, position and position error covariance matrices, since it is not enough to analyze just the moment of closest approach.

Therefore, one can divide all the methods into two main groups: linear relative motion methods and non-linear relative motion methods. In this work, we will focus on studying the latter in order to be able to estimate the collision probability of geostationary orbits .Particularly,

we will analyze one method developed by Patera [12], which is one of the most popular in the industry currently. A few realistic cases will be studied and the validity of Patera's method will be tested comparing its results with those obtained by means of Monte Carlo simulation, whose probability outputs cannot disagree in more than 10^{-4} (which is the threshold to decide whether or not performing a collision avoidance maneuver in case of collision risk)[10]. In addition, the validity of a suggested improvement of Patera's method will be tested, using the same criterion.

Prior to this study and the presentation of its results, a short background on the probability of collision calculation will be provided.

Chapter 2

Description of the problem

At an altitude of around 35786 km above the Equator, numerous satellites orbit around the Earth following a trajectory which is closed to the so-called geostationary orbit. These satellites keep always the same position with respect to the Earth's surface, a fact which is of great importance for different applications, as pointed during the introduction. Nevertheless, a problem arises when dealing with such orbit. As a simple Kepler equations derivations shows, there exists only one single Geostationary orbit. As a result, companies and states desiring to set satellites which are continuously above the Earth's surface region of interest need to place these as closed as possible to the geostationary: the further they are from this orbit, the more they will spend on fuel to make corrections in position and speed. Something that can even make the mission unfeasible.

Figure 2.1: Space Debris evolution
(Orbital Debris Quarterly News, vol. 10,issue 2, April 2006)

Among the satellites, it will be found the so-called debris with different origins: former operative satellites, material released by the satellites or natural debris. The density of debris increases and is expected to increase exponentially, as it unveils the figure 2.1 from the NASA. It should be pointed that the estimations are made based on the idealization that from to 2005, no satellites are launched: it very optimistic scenario.

2.1 Socio-economic environment

Half a century before that prediction, at the beginning of the space era,all the satellite missions and projects were led by the states. However, nowadays, more and more it is the initiative of private companies which is carrying satellite industry forward. This is what can be concluded

from the 2016 report of *The Tauri group*, which also elaborates the following plot of the growth of the satellite industry in the last ten years.

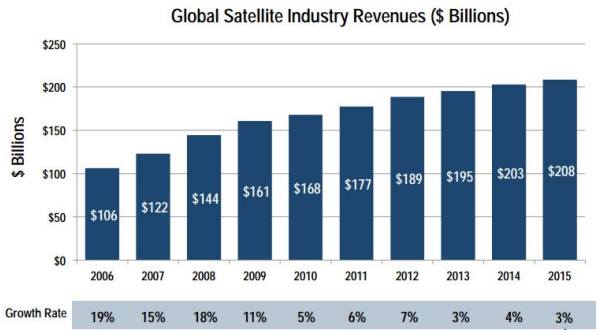

Figure 2.2: Satellite Industry Growth

Although the increase has become smother in recent times (something which is perfectly understandable after an explosive growth), this is still notable, being the growth of the industry in 2015 larger than the worldwide economic growth or the U.S. growth, with a 2.4% and a 2.5% increase, respectively. Among the different parts of such a complex industry, the GEO satellites are an important part of it. As an example of this, there were 17 orders of GEO satellites in 2015.

Certainly, the industry shows a great potential. Nevertheless, its promising future is directly linked to the capacity for allocating satellites in orbit, for which there is a room that is finite. And when it comes to taking about Geostationary Orbits, this limitation becomes clearer. Thus, anything which can improve our ability of setting satellites closer to each other will be, economically speaking, attractive. As a result, the necessity of accurately estimate the collision of probability arises; in such a way that the more confidence we may have in the probability calculation method, the smaller could be the relative distance between satellites while avoiding collisions and the formation of more debris.

Having spoken about the economic impact that the investigations on the field of probability of collision can have, let us now study the not less important social impact.

One cannot ignore when addressing this issue that many of the commodities which we enjoy in our modern societies are possible thanks to the imperative support of satellites. An extension of these services to countries or regions where they do not exist yet(or, at least, they are not as well developed) could be led by a reduction of the overall cost of a satellite, divided into three main areas: manufacturing, launching and operations. Having in principle no influence on the first two, the study of probability calculation can significantly impact the third part of the satellite life. Better estimates of the probability of collision may save costs either in terms of satellite damages due to collisions, or in terms of fuel used in unnecessary collision avoidance maneuvers.

2.2 Regulatory framework

The socioeconomic environment is not the only one that must be studied prior to enter in the pure technical work.It is clear that a knowledge of the legislation on the field of study will be needed to define the requirements of the systems to be defined and the methods to be developed. So, let us present in the lines that follow a short summary about the regulation on satellites

and the outer space.

The very nature of the outer space as well as the recentness of the orbital missions make the regulatory framework be yet to mature. From the beginning of the space exploration and conquest, the creation of laws regulating this issue has raised up many challenges: in 1957, the first artificial satellite, the Russian satellite Sputnik 1, orbited over many countries different from Russia (including the United States). If one extended the International Air Laws already current at that moment(which stated that the sovereignty of the airspace above a country corresponded to the very country) to the outer space Russia would have committed an important violation of the International Law. Nevertheless, without entering the reasons, the United States accepted the right of Russia to operate its satellite over its territory. This way, it was set that the Space Law would differ from the Air Law.

This paradigmatic example shows the difficulty of the creation of Laws concerning the Space Law. Therefore, what has been regulated up to date is not much. Nevertheless, there has been many efforts to improve this situation, based(as could not be otherwise, due to the very nature of the orbital space) on international treaties. These define general principles with which National Laws must comply with. Among all the treaties, it is compulsory to highlight the *Outer Space Treaty(1967)*, which sets the basis of the international space law.

In addition, UN(with its specialized office UNOOSA) as well as other supranational organism such as the ESA issue documents to which countries generally adhere, although they are non-compulsory. It must be mentioned as well the ITU(International Telecommunication Union, agency of the UN) which is in charge of addressing the conflicts that arises for the allocation of satellites in Geostationary Orbit, at which there exits a regulated maximum number of slots.

In effect, the regulations were and still are effective to avoid disputes and tensions among countries regarding the space. However, they lack of accuracy in topics that are more and more important as time passes. In particular, the topic that is the concern of this work is insufficiently treated. On one hand, about the space debris formation and its consequences, there is not a defined liability in case of accident or collision. On the other hand, regarding technical aspects, there is not a common standard to avoid the formation of new debris. The IADC (Inter-Agency Space Debris Coordination Committee) proposes some guidelines for the mitigation of space debris[5], in which the topic of collision probability is mentioned as a way of limiting the creation of debris. However, it is always treated in a qualitative way:

"If reliable orbital data is available, avoidance manoeuvres for spacecraft and co-ordination of launch windows may be considered *(*if the collision risk is not considered negligible)"

This absence of quantitativeness can be due to the immaturity of the field from a technical point of view. Nevertheless, in future years, with the technical development on this area; and forced by the increase of private companies wishing to set their satellites on orbit, and the fact that the increase in debris population may make eventually impossible to keep on setting satellites on Earth orbit, the regulation will be significantly improved setting qualitatively limits.

2.3 Definition of encounter. Short-term vs. Long-term

Among the tasks of the regulatory agents, there is for instance that of setting a maximum for the proximity of two orbiting bodies. Indeed, it is the proximity,as well as the similarity, of the orbits described by the satellites in GEO which leads to the bodies eventually being relatively closed one to each other(mainly when there exists the formation of debris) during a significant fraction of the time to complete one orbit. This is what is defined as a long-term encounter.Opposed to it, as briefly remarked in the introduction, there is the short-term encounters.

Let us then address the definition of encounter, which is of paramount importance for further developments in this work. The term encounter is inevitably related with the existence of uncertainties in the determination of the position of the satellites. The impossibility to perfectly track the motion of the orbiting bodies creates the need to estimate the uncertainty associated to the tracking, which defines an error-probability density ellipsoid, normally distributed, centered at the tracked satellite position. In order to completely define the ellipsoid, there is still the need to decide how many standard deviations are to be considered. The common choice (and the one used throughout the work) is 3 standard deviations, which defines a confidence interval of 97.07% in three dimensions, although larger values may also be chosen. Although further explanations will be given about the error ellipsoid in the following section, it must be said at this point that the term error covariance matrix refers to the analytical expression of the error ellipsoid(together with the mean if the distribution is Gaussian), and that both terms may be used interchangeably along this work.

Now, each satellite has its associated error ellipsoid in the local reference frame. After transforming each ellipsoid to the inertial reference frame (considering the Earth fixed reference frame as inertial), they are summed accounting for the possible correlation between both ellipsoids. Then, the resulting combined 3D position error ellipsoid is centered at one of the orbiting bodies (let us call it satellite 1, and satellite 2 the other). And here is where the definition of encounter comes forth: an encounter extends as long as the satellite 2 is inside the 3σ combined position error ellipsoid centered at satellite 1.

Having defined clearly this important term, it is feasible to explain accurately the difference between short term and long term encounters. Let us imagine firstly two bodies in orbits which are in different orbital planes. If they eventually happen to come relatively near to each other, in other words, if they have an encounter, it is easy to see that this will occur at very high speed, and as a result, the satellite 2 will be a small fraction of time(compared to the period of the orbit) inside the ellipsoid centered at satellite 1. The encounter will look as in picture 2.3

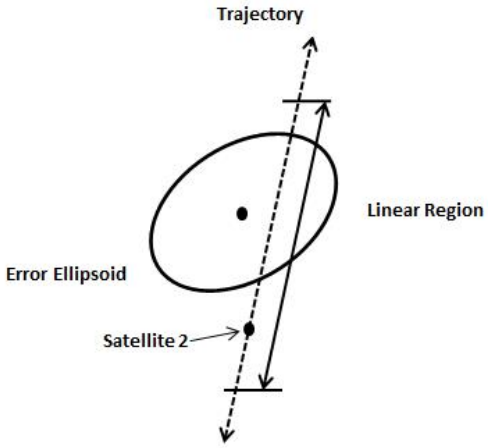

Figure 2.3: Linear Encounter

Given that the encounter is "short enough", velocity and position error ellipsoid are roughly constant throughout it. Then, the error ellipsoid volume swept by the orbiting body B is nothing but a straight tube with cross-section the shape of the satellite projected in a plane perpendicular to the relative velocity direction. This permits great simplifications in the calculations. For instance, Patera proposes a method in which, after decoupling the probability density along each axis by scaling the error ellipsoid, he extends the mentioned tube from $-\infty$ to $+\infty$, introducing a negligible error since the error ellipsoid already accounts for 97.07% of the probability. Then, along the velocity direction, the integral of the density function equals 1 and the problem reduces to make a single area integral in the plane perpendicular to the velocity of the tube cross-section at the point of closest-approach. Other methods exist that take advantage of the fact that the relative velocity in the encounter can be considered linear.

Contrary to what happens in linear motion or short-term encounters, there is the case of 2 satellites orbiting in more or less the same orbital plane and with similar eccentricities. As a consequence, one cannot calculate the probability of collision by simply propagating to the point of closest approach and making the integral of the cross section. Now, the value of the relative velocity becomes important and the integration of the error ellipsoid volume swept by the hardbody is not an easy task. This is what occurs with satellites in GEO orbit and , as in the case of short-term encounters, there are several methods in the literature[2][9][3]. Patera's method is the one that will be studied.

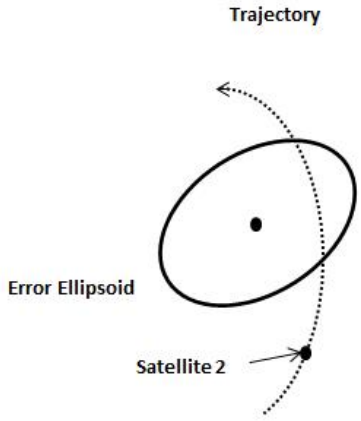

Figure 2.4: Non-linear encounter

2.3.1 Error ellipsoids

As seen in the previous section, the position error ellipsoid is a key element of the process of calculation of the probability of collision. Thus, it is certainly worth discussing about its origin and main features, which may be useful to know in future sections of this work. Velocity uncertainty is considered negligible, as it is done in Patera's method and other well-known probability tools.

Evidently, the error ellipsoids come to play a role in the concerning problem due to the fact that there exists certain uncertainty regarding the position and velocity of the orbiting bodies at a given time t. This uncertainty can be identified as coming from 2 main major sources:

- **Measurent errors**: As the very name indicates the measurement errors are caused by the fact that there exist some inaccuracies in the observations such as operator errors, equipment failure, the very limitations of the tracking sensors...
  If the calibration of the instrument of measurement is not rightly done, we might end up having a type of error called *bias*, which consists of a constant offset from the true value. When the measurements are scattered around a mean value, the error is called *noise*. Furthermore, there still exists an error which is called *drift* being this a variation over time of the observed mean.

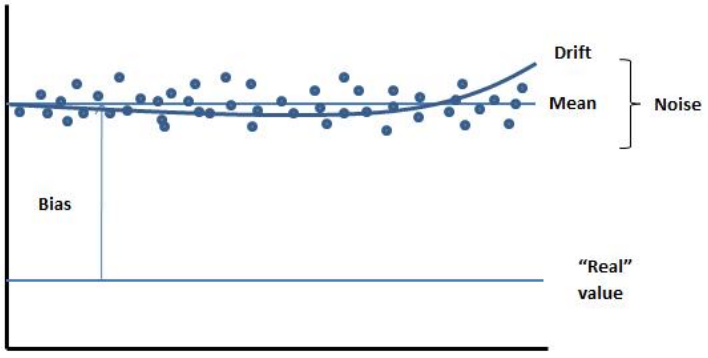

Figure 2.5: Noise, Bias and Drift

What is concerning the problem of interest, both biased and drift are assumed to be zero, in such a way that only noise error exists. Out of this error, the ellipsoids will be built up after a certain processing of the data, which will be discussed later in this section.

- **Modeling errors**: The mathematical models used to describe the motion of the satellite are not perfect. There will be as a result an uncertainty in the propagation of the satellite state vector, which is called process noise, being mainly consequence of the inexactness of the Earth's gravity field modeling, and the atmospheric drag effect. The latter is a major source of uncertainty whose effect, fortunately, shall not be considered in this work since the Geostationary satellites orbit at an altitude much larger than 1000 km, which is considered to be the boundary upon which the solar radiation pressure effect has more influence than the atmospheric drag.

The first type of uncertainty, the one depending on the measurements quality, is evidently present in the tracking of the satellite. It has already been said that the only measurement error is noise. Thereafter, if one assumes that the noise is the result of several independent causes which randomly affect the observations, the Central Limit Theorem states that the distribution of these same observations if they are numerous enough, will tend to be normal, this is, Gaussian. Then, the application of a certain estimation scheme, e.g. Kalman filter or Least Square, yields an error ellipsoid, E_e with a 3D Gaussian distribution, expressed analytically by a mean vector and a error covariance matrix.

$$E_e \equiv \{\vec{x}_{mean}, \overline{\overline{C}}\} \tag{2.1}$$

where $\overline{\overline{C}}$ is a 3x3 positive definite matrix which, in the case of the principal axis of the ellipse being aligned with the axes of reference, looks like this:

$$\overline{\overline{C}} = \begin{bmatrix} \sigma_x^2 & 0 & 0 \\ 0 & \sigma_y^2 & 0 \\ 0 & 0 & \sigma_z^2 \end{bmatrix} \tag{2.2}$$

One might also consider a last type of error: the actuation error. This refers to the difference that exists between the commanded actuation (in terms of magnitude and direction) and the actual actuation.
Finally about the errors, for a further understanding of their nature, it is possible to divide them into two main groups, as suggested by the referenced paper[7]: aleatory errors and epistemic errors. Into the first group would fall the measurement and actuation errors, characterized as they are by being inherent to the physical system. One must simply adapt to them. Contrarily, the epistemic error, to which the model error belongs, depends on the degree of comprehension that exists on the physical system, and can be reduced after an effort for improving the model.

Ellipsoid propagation

In the previous subsection, the initial error ellipsoid was defined. Once this has been done, it arises the need to propagate it over time. This propagation is given by the following expression:

$$\dot{C} = \frac{\delta F}{\delta t} C + C \left(\frac{\delta F}{\delta t} \right)^T + Q \tag{2.3}$$

being F a function such that for any time t,

$$\dot{x} = F(x, t) \tag{2.4}$$

and Q is the previously mentioned *process noise*, due to errors in the dynamic model, this is, in F. It should be noticed that the covariance rate of change over time depends on the very initial covariance matrix as well as in the error of the model. Indeed, this is something that can be intuitively got. If the initial position of the satellite is not the "real" one, even if the velocity is perfectly known, the initial orbit determination will yield incorrect orbital elements(e.g. eccentricity, angular momentum...). This error will grow as time passes from the moment of the observation. In addition, if one perfectly knew the initial position and velocity, there would be still a certain uncertainty produced by Q, the errors in the model.

Error Covariance matrix transformation

Along the process of propagation of the satellites' states as well as during the implementation of Patera's method, the need for transforming the covariance matrix will arise several times. Therefore, We should not go forward before having defined how this transformation is done.

One must firstly have in mind the mathematical definition of covariance matrix, which is

$$C = \mathbf{E}[(X - \mathbf{E}(X))(X - \mathbf{E}(X))^T] \tag{2.5}$$

Now, if we call X'=X-$\mathbf{E}$(X), a transformation M, such as a rotation, to the vector X' is applied as follows:

$$X'_{trans} = MX' \tag{2.6}$$

Then,

$$C_{trans} = \mathbf{E}[MX'X'^T M^T] \tag{2.7}$$

And finally, since the matrix M entries have no uncertainty, their expected values are themselves.

$$C_{trans} = M\mathbf{E}[X'X'^T]M^T = MCM^T \tag{2.8}$$

As said before, we will come back in next sections to this result.

2.4 State of the art

Many papers have been written dealing with the problem proposed in the lines that preceded this section. Yet, only the most important among them will be briefly explained here with the goal of building a modest but accurate portrait of the current situation.
One of the first methods developed aiming at tackling the non-linear problem was the one of Patera, therefore, the methods that are to be presented here are subsequent. Indeed, some of them make use of the original idea of Patera, as it will be seen now. Finally, it should be pointed out that the fact that this methods come after Patera does not necessarily mean they yield better results.

2.4.1 Mahalanobis distance metric

The first method to be introduced yields, unlike the rest of the approaches to be analyzed, an instantaneous metric. This means that it measures "the instantaneous probability of collision as function of time", as defined in [14]. It is interesting because it sets an upper limit to the total probability which, opposed to the instantaneous probability of collision, gives us the cumulative probability of collision over a certain time t.
Although it will be precisely defined in the methodology section, it should be said briefly that the Mahalanobis distance measures how many standard deviations of a certain statistical distribution separate two objects. Dimensionless as it is, the value of the metric is directly the minimum value of the Mahalanobis distance over the period in which one wants to calculate the total probability of collision.

$$p_{ins} = min_{t_0<t<t_f} \left(\frac{d}{\sigma} \right) \tag{2.9}$$

where d is the distance between the satellites and σ is the standard deviation of the combined error ellipsoid in the direction of the line that joins both satellites. Noticing the simplicity of the metric, it is clear that the main advantage of the method is its short computational time. Nonetheless, many times, the metric will be found to be very conservative, which is not good, because it will lead us to perform unnecessary collision avoidance maneuvers.

2.4.2 Mckinley's adjoining tubes

In the same way as the previous method, the method of Mckinley is similar to that of Patera. In effect, the author proposes a small variation in the method. Without introducing yet the method of Patera, it should be mentioned that Patera proposes a discretization of the trajectory of the satellite in such a way that for each time step the satellite trajectory sweeps a volume which is that of a cylinder. Then, what Mckinley varies with respect to Patera's approach is that he transforms the cylinders into adjoining tubes avoiding the gaps and overlaps in order to represent with a higher fidelity the trajectory of the satellite. This method could be interesting for relatively large size satellites compared to the size of the error ellipsoid (for reasons that will be given in the Methodology part).

2.4.3 Chan's analytical approach

Unlike in the rest of methods previously seen, Chan develops an analytical solution. *A priori*, it may seem attractive. However, the analytical solution is particular for an orbit and as a result, it must be recalculated when the orbit characteristics change. This fact may make it inefficient.

Other methods have been also developed, but it has been thought to be enough to introduce a few of them (believed to be the most significant one), being the rest less important, similar to ones already introduced, or even being methods of a different nature.

The expression "methods of a different nature" makes reference to those probability calculation tools which consists of an improvement of the method of Montecarlo, aiming at making it more efficient by reducing the huge computational time associated to it. Detailed explanations on this method will be given in the next section. Nevertheless, we would like to cite some papers which reduces significantly the computational time of the Montecarlo simulation

for the particular case of satellite collisions [6][14]. This reduction, although not large enough to compare with the efficiency of the method of Patera, is of great utility since the method of Montecarlo is used as reference to check the validity of Patera. Thus, computational time reduction in Montecarlo has reduced hours of simulation time during the realization of this work.

2.4.4 Modern uncertainty propagation techniques

The previous methods do not say anything about the propagation of the error ellipsoid. However, as it will be seen lately, this is not a minor issue on the calculation of collision probability. Indeed, the changes that occur to the error ellipsoid are significant in a time span, for instance, of one orbital period. For this reason, numerous method have been developed to try to solve the problem of propagation of uncertainty without having to turn to the costly and time-consuming Montecarlo. They can be divided into linear and non-linear propagators:

Linear uncertainty propagators

The linear propagators linearize either the dynamics or the probability function. An example of the former are the *Local Linearization methods*, which, by means of a first order Taylor expansion linearize the nominal trajectory(the one obtained assuming no uncertainty). Then, the mean and the covariance are propagated linearly with a matrix named State Transition Matrix, as follows:

$$m(t) = \Phi(t, t_0)m(t_0) \tag{2.10}$$

$$C(t) = \Phi(t, t_0)C(t_0)\Phi^T + G(t)Q(t)G(t)^T \tag{2.11}$$

where the State Transition matrix is Φ, and G and Q are a matrix characterizing the diffusion process and a covariance associated with Brownian motion process, respectively.

Instead of linearizing the dynamics, one might statistically linearize the problem. This is what is done in the *Statistical Linearization Methods*. They define an epproximation error:

$$e(t) = f(x, t) - f'(x, t) - Nx \tag{2.12}$$

and they try to choose f'(x,t) and N in order to minimize the mean square of the approximation error, $J = [e^T Se]$

Non-linear uncertainty propagators

Many non-linear propagators have been developed as well to overcome the deficiencies of linear propagation techniques. The first that could be mentioned is the *Unscented transformation*, which consists of deterministically choosing points (called sigma points) on the initial uncertainty cloud and propagating only these points to generate a transformation function at a given time t. Evidently, this set of points must fulfill that their mean and variance is the same as the original distribution. In addition, the influence of the sigma points on the transformation function is weighted as:

$$m(t) = \sum_{k=1}^{P} \omega_k x_k(t) \tag{2.13}$$

$$C(t) = \sum_{k=1}^{P} \omega_k [x_k(t) - m(t)][x_k(t) - m(t)]^T \tag{2.14}$$

where P refers to the number of sigma points chosen. Now, in order to select the weights there exist numerous techniques, not an unique solution.

Unlike in the *Unscented transformation method*, in the *Polynomial chaos* propagation method higher order moments than the mean and variance can be propagated; something which can be very useful when the random variable of analysis is not Guassian. The foundational idea of this propagator is that of approximating the output random variable as a sum of polynomials as:

$$\mathbf{x}(t, \epsilon) \approx \sum_{k=0}^{P} c_k(t) \Phi_k(\epsilon) \tag{2.15}$$

In this equation, ϵ represents the multivariate random input, Φ_k a polynomial and $c_k(t)$ the coefficient at a given time t. And again, as it occurred with the previous method, there exist numerous techniques for obtaining the coefficient and the polynomials. The main drawback of Polynomial chaos is its inefficiency when the dimensionality of the problem increases.

A very different method to the two previously introduced is the propagation by *State Transition Tensor*. This can be summarized as being an extension of the linearization methods, in the sense that it takes higher order terms of Taylor expansion. It is a semi-analytical method, and it has as main drawback its great complexity.

Other important methods in propagation of uncertainty are those based on *Differential algebra*[8]. Given the lack of rigor which suffers derivatives to model functional dependence, this technique was developed to compute the derivatives of functions with computers.

And last, but not least, it is worth mentioning the technique called *Gaussian mixture model*, which, motivated by the fact that, in orbital propagation, the initial Gaussian distribution might eventually end up by being non-Gaussian, tries to approximate an arbitrary random distribution by a sum of weighted Gaussian probability density functions. This is,

$$p'(t, \mathbf{x}) = \sum_{i=1}^{N} \omega_i p_g(x_i; m_i, C_i) \tag{2.16}$$

where p_g is a Gaussian probability distribution and p' is the target probability distribution.

Finally, other techniques exit which can be hardly classified as linear or non-linear, such as the *Change of coordinates* technique, which is based on the fact that there are coordinates bases which are better than others for propagation of uncertainty purposes.

Chapter 3

Methodology

3.1 Case study

After having defined the problem that this work is to dealt with, there is the need to specify which concrete orbital motion cases will be analysed with the goal of extrapolating the results to other orbital motion of geostationary satellites. For practical purposes, as a way to validate the method, the cases are similar to the ones implemented in the paper of Patera [12]. In addition, they all are for a time span equal to one orbital period(one day in GEO), since this is interesting from the point of view of collision avoidance maneuver.

The first of them consists of two satellites in the Geostationary orbit, at a distance of 1000m in track (see figure 3.1). At $t = 0$; one of the satellites (satellite 2) gets an increment on velocity which is radial, and which makes it gain some eccentricity on its movement. Both orbiting bodies are considered spheres, looking for eliminating the problem of having to deal with satellite attitude; and the combination of both satellite bodies is referred to as the so-called *hardbody*. The sum of their radii is 50 m. Finally, the initial error ellipses are spheres and the sum of their standard deviations is 1 km. The parameter ΔV will be varied along the study. Notice that this velocity increment does not represent a thrust impulse in a collision avoidance maneouver. Its purpose is simply that of building the different satellite trajectories with its variation. This will hold for the two first case studies, not for the third one, as it will be seen later.

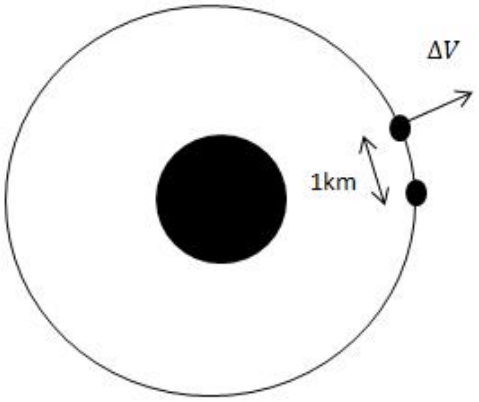

Figure 3.1: First case study, at t=0

During the methodology section, only this first case study will be developed, since the procedure is analogous for the rest of cases that will be studied. This will hold as far as there is not any particularity of a given case.

The second case to be analyzed is that of two satellites in circular orbits with different radii, both in the equatorial plane. The sum of the satellite radii as well as the error ellipsoid sizes are the same as in the previous case. However, this time, the ΔV applied to the satellite in the largest radius orbit, is not radial, but tangential to the trajectory, and opposed to the satellite orbital speed. It should be pointed that this case, although simulates a long term encounter, does not correspond to a situation in GEO: the radii of the orbits are smaller. Nevertheless, the conclusions whose analysis may lead us to can be extrapolated to GEO, since the orbit shapes are similar.

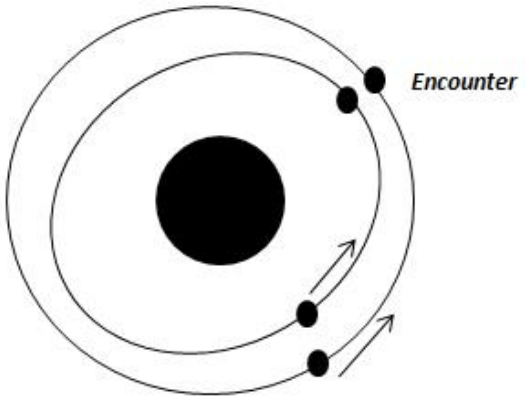

Figure 3.2: Second case study

Finally, the third study case is defined to apply the knowdelege previously adquired from the other cases to a collision avoidance maneouver situation. The case is defined in the following way: firstly, the two satellites are placed in the same position and they are propagated back in time half the orbital period. Then, the output of the propagation is used to define the initial conditions for the third case study, in such a way that if there is no ΔV at $t = 0$; then, satellites will get to exactly the same position after a time equal to half a day. Thus, it will be with $\Delta V = 0$ that the probability of collision will be maximum, and this will decrease as the velocity impulse increases. Now, it is understand why this time ΔV can be interpreted to be a thrust impulse in a collision avoidance maneuver.

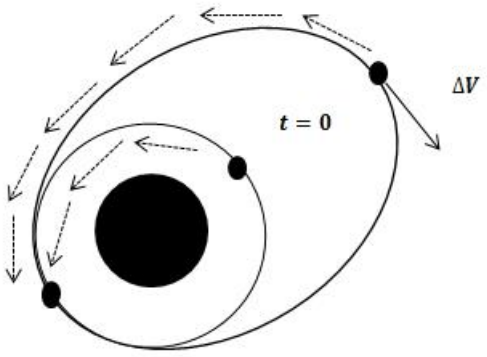

Figure 3.3: Third case study

3.2 Choice of the dynamic model

It is of great importance for the trade-off between accuracy and computation time to make the right decision when selecting the dynamic model to be inputted to the algorithm of probability computation. In the literature about the subject, two different classical dynamic models are typically used, and so, they will be studied in this section, in increasing level of fidelity to the real motion (with the penalty of computation time). They are Clohessy-Wiltshire approximation, Kepler model. It should be added that a further analysis would include the orbital perturbation model C_{22}, but according to Patera[12], for probability computation purposes and a time of one day, the mentioned model is not needed. Once this point has been made, let us proceed now introduce the models to be studied.

The so-called Clohessy-Wilstshire approximation provides an analytical solution to the problem of relative motion between two orbiting bodies. It is a simplification of the already simplified equations of linear relative motion obtained by stating that $\frac{\delta r}{R} << 1$, where δr is the relative position vector norm and R is the distance from the Earth centre to the orbiting body taken as reference. What is particular in Clohessy-Wiltshire is that the satellite 1 has a circular orbit. This, added to the previously mentioned simplification, permits us to obtain a set of linear differential equations, which are solved analytically, reducing significantly the computational time compared to the two other methods that will be exposed. These equations are of great utility in case of certain rendez-vous maneuvers.

$$\{\delta r(t)\} = [\Phi_{rr}(t)]\{\delta r_0\} + [\Phi_{rv}(t)]\{\delta v_0\} \tag{3.1}$$

$$\{\delta\} v(t) = [\Phi_{vr}(t)]\{\delta r_0\} + [\Phi_{vv}(t)]\{\delta v_0\} \tag{3.2}$$

where

$$[\Phi_{rr}(t)] = \begin{bmatrix} 4-3\cos(nt) & 0 & 0 \\ 6(\sin(nt-nt)) & 1 & 0 \\ 0 & 0 & \cos(nt) \end{bmatrix} \quad [\Phi_{rv}(t)] = \begin{bmatrix} \frac{1}{n}\sin(nt) & \frac{2}{n}(1-\cos(nt)) & 0 \\ \frac{2}{n}(\cos(nt)-1) & \frac{1}{n}(4\sin(nt)-3nt) & 0 \\ 0 & 0 & \frac{1}{n}\sin(nt) \end{bmatrix} \tag{3.3}$$

$$[\Phi_{vr}(t)] = \begin{bmatrix} 3n\sin(nt) & 0 & 0 \\ 6(\cos(nt-1)) & 0 & 0 \\ 0 & 0 & -n\sin(nt) \end{bmatrix} \quad [\Phi_{rv}(t)] = \begin{bmatrix} \cos(nt) & 2(\sin(nt)) & 0 \\ -2n\sin(nt) & (4\cos(nt)-3) & 0 \\ 0 & 0 & \cos(nt) \end{bmatrix} \tag{3.4}$$

Nonetheless, the presence of some secular terms in the linear equations as well as the fact that during the relative motion of the satellites the condition $\frac{\delta r}{R} << 1$ might not hold true may lead us to think that the model will not be good enough for times of the order of the orbital period in GEO.

Given this expected lack of accuracy of Clohessy-Wilstshire, a less simplified model is used to propagate the satellite through time on its orbit, Kepler's. The equations derived by the German scientist are well-known in celestial mechanics, and their application consists of, determining firstly the orbital parameters through the initial state data obtained by means of the tracking of the satellites, and secondly, with the just obtained parameters of the orbit, getting for each

satellite the state at any time t.

$$\vec{x}_0(t_0) \rightarrow \{h, e, \upsilon, a, p...\}; \qquad \{h, e, \upsilon, a, p...\} \rightarrow \vec{x}(t) \tag{3.5}$$

where $\{h, e, \upsilon, a, p...\}$ are the minimum necessary parameters to define an orbit.

3.3 Patera's Method

Relying on the dynamic model chosen for the propagation, the method of Patera is able to output an estimation of the non-linear collision probability. Now, in the lines that follow, the main features of the algorithm are explained.

Inputs

It is important, prior to giving any further detail on the implementation of the method, to specify the inputs of the probability calculation algorithm.

The dynamics of the two bodies of analysis are the first inputs. The dynamic model will be subject of discussion in the results section.

Another input is the uncertainty of the position of the satellites. This uncertainty is contained within the position error covariance matrices, which were analyzed in detail in section 2.3.1 . These uncertainty matrices must be rotated as the satellite travels on its orbit, given that they keep diagonal in the body-fixed reference frame. In addition, the correlation between the two matrices is typically assumed to be zero,since at the Geostationary orbit, the main cause of uncertainty correlation(the atmospheric drag), has no influence on the satellites.

Finally, the program requires the shape of the bodies of analysis. Typically, in order to be conservative and avoid additional computational effort, the shape of the bodies is assumed to be a sphered centered at the centre of the mass of the satellite and radius equal to the largest distance possible from the centre of mass to a point in the profile of the body. Hereafter, thanks to this assumption, no attitude information is required.

Methodology: transformations

Once the inputs are obtained, the very first step of the method is just transforming the covariance position error ellipsoids (given in the form of 3-by-3 matrices) from the local frame of reference in which they are given to the Inertial frame of reference.

$$C_{1I} = P_1 C_1 P_1^T \tag{3.6}$$

$$C_{2I} = P_2 C_2 P_2^T \tag{3.7}$$

Subsequently, the ellipsoids in the same frame of reference and, as discussed before, considered to be uncorrelated, can be summed analytically by simply adding the matrices:

$$C_T = C_{1I} + C_{2I} \tag{3.8}$$

At this point, it must be said that the combined covariance matrix is centered at the satellite 1. Now, the combined ellipsoid is transformed into a space in which the 3D object becomes a sphere (the purpose of these operations will be exposed afterwards). This is done in two step:

$$C_{Td} = QC_TQ^T = \begin{bmatrix} \sigma_1^2 & 0 & 0 \\ 0 & \sigma_2^2 & 0 \\ 0 & 0 & \sigma_3^2 \end{bmatrix} \tag{3.9}$$

where Q^T is the matrix whose columns are the eigenvectors of the matrix C_{Td}. Then,

$$C_{Ts} = SC_{Td}S^T = \begin{bmatrix} \sigma_1^2 & 0 & 0 \\ 0 & \sigma_1^2 & 0 \\ 0 & 0 & \sigma_1^2 \end{bmatrix} \tag{3.10}$$

being S

$$S = \begin{bmatrix} 1 & 0 & 0 \\ 0 & \frac{\sigma_1}{\sigma_2} & 0 \\ 0 & 0 & \frac{\sigma_1}{\sigma_3} \end{bmatrix} \tag{3.11}$$

The frame to which the error ellipsoid has been transformed is called scaled frame. There is only one transformation left, to a space which is defined by the relative position and velocity vectors in the scaled frame: the encounter frame.

$$X = r_2 - r_1 \tag{3.12}$$

$$V = u_2 - u_1 \tag{3.13}$$

Then, in the scaled frame:

$$X_S = SQX \tag{3.14}$$

$$V_S = SQV \tag{3.15}$$

The way the encounter plane is defined is as follows (see figure 3.4): the z-axis parallel to the relative velocity vector in the scaled frame, the y-axis perpendicular to the plane of motion, and the x-axis completing the right-hand rule system.

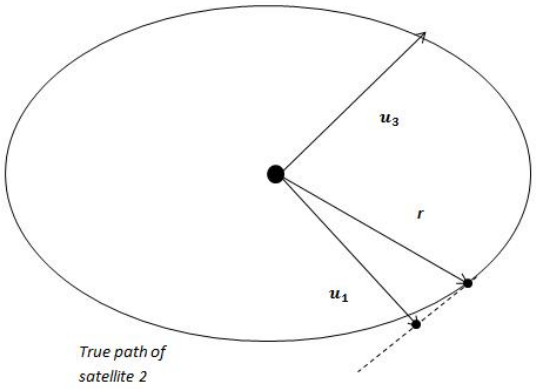

Figure 3.4: Relative path of satellite 2, definition of the encounter frame

Let us then transform the combined error position ellipsoid to the encounter frame through the matrix W:

$$C_{Te} = WC_{TS}W^T \tag{3.16}$$

Notice that the matrix W is orthogonal and C_{TS} is symmetric $C_{Te} = C_{TS}$. Finally, prior to starting with the probability computation, it is necessary to transform the volume to transform the combined hardbody volume (obtained by adding the spheric volumes defined for each satellite) of the satellites to the encounter frame.

$$f_{ie} = WSQP_2 f_i = Uf_i \tag{3.17}$$

being f_i any point of the combined hard-body surface. Notice that the combined hardbody radius is to be centered in the orbit of satellite 2, this is why we use P_2 in equation 3.17 .

Methodology: calculation of probability

Just at the very first step of the probability calculation, it comes forth the motivation behind transforming the error ellipsoid into a sphere. The integration of the Gaussian probability density over the volume swept by the hardbody function can be written as:

$$PR_t = \frac{1}{(2\pi)^{3/2}\sigma_1^3} \iiint_{Vol} exp\left[\frac{-(x^2+y^2+z^2)}{2\sigma_1^2}\right] dx\, dy\, dz \tag{3.18}$$

where the probability density along one axis is decoupled from the other two axes. This fact facilitates importantly the calculations. Let us now transform the integral into cylindrical coordinates, aligning z, this is, the velocity direction in the encounter frame, with the cylinder axis.

$$PR_t = \frac{1}{(2\pi)^{3/2}\sigma_1^3} \iiint_{Vol} exp\left[\frac{-z^2}{2\sigma_1^2}\right] exp\left[\frac{-r^2}{2\sigma_1^2}\right] r\, dr\, d\theta\, dz \tag{3.19}$$

Now, this transformation is done in order to define the differential probability, per unit of length in the velocity direction, which is defined as:

$$PR_I = \frac{\Delta z}{(2\pi)^{1/2}\sigma_1} exp\left[\frac{-z^2}{2\sigma_1^2}\right]\left(\frac{1}{2\pi}\right) PR_C \tag{3.20}$$

being PR_C the integral of the surface perpendicular to the velocity direction, which will be defined afterwards. Now, if this expression is divided by the increment in time during which the distance Δz is traveled, one gets the rate of collision probability, assuming that the speed is constant during the differential time:

$$PR_R(t) = \frac{V_z}{(2\pi)^{1/2}\sigma_1} exp\left[\frac{-z^2}{2\sigma_1^2}\right]\left(\frac{1}{2\pi}\right) PR_C \tag{3.21}$$

Finally, PR_T(total probability) is obtained by numerical integration of:

$$PR_T = \int_{t1}^{t2} PR_R(t)dt \tag{3.22}$$

The time step dt will be determined in the usual manner, which consists of decreasing the time step until a convergence in the results with different time steps is observed. Evidently, the selected value of dt will be dependent of the geometry of the relative motion of the two

satellites. The more curved the trajectory is, the smaller should be the time step. In general, with several hundred of time steps per orbit is enough.

Let us, before continuing with the methodology, highlight a geometrical consideration of the method which is the consequence of the step taken between equation 3.19 and equation 3.20: the infinitesimal length dz turns into a non-infinitely small length named Δz. Thus, the geometrical consideration is nothing but pointing that the volume swept by the combined hardbody in the error ellipsoid is composed by small adjacent tubes, whose combination will leave gaps and overlaps.

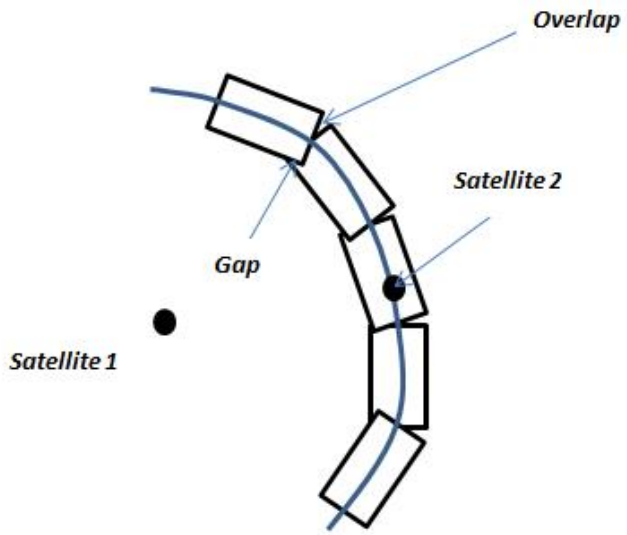

Figure 3.5: Adjacent tubes, with gaps and overlaps

These gaps and overlaps, represented in figure 3.5, seem to clearly worsen the quality of the method of Patera. However, Patera states that given that the gaps and overlaps represent very closed probability volumetric regions in the error ellipsoid, the effect of one counteracts the contribution of the other. This assertion implies that one does not need to decrease the size of the tubes as much as in the case of the gaps and overlaps affecting significantly the probability computation; in such a way, the computational time is also importantly reduced.

Contour integration

The previously mentioned surface integral PR_c is worthy of further precision at the description. As said before, this is the integration of the 2 dimensions of the hardbody(transformed to the encounter frame) in the direction perpendicular to the speed. The integral to be performed is:

$$PR_C = \iint exp\left[\frac{-r^2}{2\sigma_1^2}\right] r\, dr\, d\theta \tag{3.23}$$

with the center of the combined error ellipsoid, this is, the center of the satellite, being the origin of coordinates of the plane of integration.
Then, there are two posibilities, if the combined hardbody on the encounter plane happens to

encircles the center of coordinates, then:

$$PR_C = \oint_{perimeter} \left(1 - exp\left[\frac{-r^2}{2\sigma_1^2}\right]\right) d\theta \simeq 1 - \sum_{i=1}^{n} exp\left[\frac{-X_i^2 + X_{i+1}^2}{4\sigma_1^2}\right] d\theta_i, \tag{3.24}$$

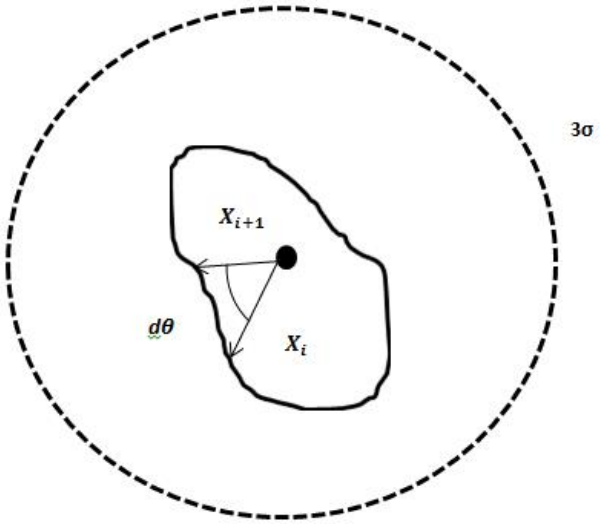

Figure 3.6: Contour intergration, center encircled

whereas if the combined hardbody does not encircle the origin, we have:

$$\begin{aligned} PR_C = \oint_{perimeter} \left(exp\left[\frac{-r_1^2}{2\sigma_1^2}\right] - exp\left[\frac{-r_2^2}{2\sigma_1^2}\right]\right) d\theta \simeq \\ \simeq \left(\sum_{i=1}^{n} exp\left[\frac{-X_i^2 + X_{i+1}^2}{4\sigma_1^2}\right] - \sum_{j=i}^{n} exp\left[\frac{-X_j^2 + X_{j+1}^2}{4\sigma_1^2}\right]\right) d\theta_i, \end{aligned} \tag{3.25}$$

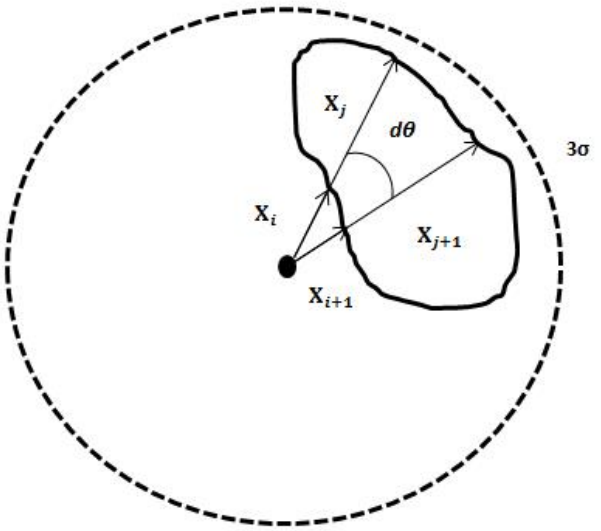

Figure 3.7: Contour integration, center not encircled

3.4 Montecarlo simulation

As mentioned along the description of the problem, the Montecarlo simulation will be taken as a reference to which compare the results obtained from the method of Patera. The reason why Montecarlo's output is used as a value of reference will be better comprehended after the explanation of the method bases.

The simulation of Montecarlo reliability lies on the so-called Law of Large Numbers. Thus, the process consists basically on randomnly generating a large number of inputs which will yield the same number of random outputs whose expected value is the desired result. Or mathematically speaking,

$$p = \frac{1}{n}\sum_{i=1}^{n} H(X) \tag{3.26}$$

where p is the probability and $H(X)$ is the output of a given function whose input is a random variable following a random distribution. p is also known as Montecarlo estimator, and

$$\lim_{n\to\infty} P(|p - E(H(x))| < \epsilon) \tag{3.27}$$

for an arbitrarily small value of ϵ is the Law of large numbers applied to the estimator.

After this brief introduction to the method, the question to be addressed now is how to particularize it for the problem which concerns us.
Let us firstly define which is the input of the simulation, the mentioned random variable in equation (3.26). This is clearly the relative position of the orbiting bodies before propagation. These positions are randomly generated following a normal law (since this is the error density distribution followed by the position error ellipsoid) with mean and variance those of the ellipsoids. The velocity uncertainty is considered negligible, as in Patera's method.

Then, what follows is the propagation of the initial satellites states obtained through the random generation. The propagation is made through the dynamic models explained in section 3.2.

Now, notice why the method of Montecarlo is used to check the validity of others: no assumptions on the propagation of the error ellipsoids are made, something which is one of the hardest issues on probability of collision calculation. Certainly, the precision of the method only depends on the quality of the satellites track and the error estimations, as well as the model precision; which are just the inputs to the probability calculation algorithm(although without, not easy to get accurately). Thus, as far as the inputs are precise, the Montecarlo simulation will yield the "true" result,if n is large enough.

The issue of n being "large enough" is key for further developments Montecarlo used during this project, yet, the explanation of the methodology has not still finished. We had already mentioned the propagation: this is done up to the point of closest approach. Then, if the miss distance(the distance at the point of closest approach) between the center of the satellites is smaller than the radius of the combined hard-body, there is a collision, if not, there is no

collision. Therefore, one can define the function $H(X)$

$$H(X) = \begin{cases} 1; & \text{if } d_{miss} < r_{hard-body} \\ 0; & \text{if } d_{miss} > r_{hard-body} \end{cases} \tag{3.28}$$

where, as said before, $X \sim f(x)$, being $f(x)$ a normal law. Then, run after run this process is repeated, adding a one to the sum in equation 3.26, and finally, dividing the result by the total number of runs, we get the Montecarlo estimator.
Finally, it should be noted that as in the method of Patera, the precission of Montecarlo is associated with the number of time steps. Certainly, the shorter is the time that separates the evaluations of equation 3.28, the more accurate will be the output value of the simulation.

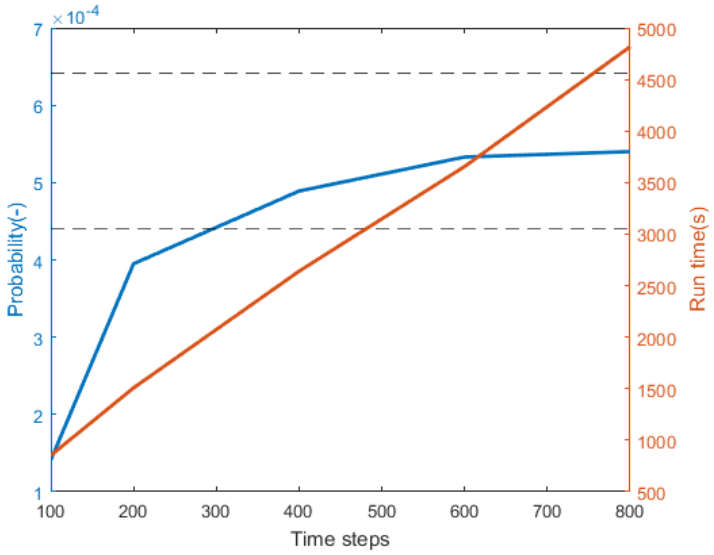

Figure 3.8: Convergence vs time step number

With the margin of 10^{-4}, the convergence of the solution is checked and a number of time steps of 400 is taken as accurate enough. The picture shown is for a $\Delta V = 0.3m/s$

3.4.1 Importance Sampling

The main drawback of Montecarlo is the computational time associated to the simulation. As said some lines above, to ensure a small variance in the Montecarlo estimator, the number of runs must be large enough, which is usually a large number of simulation and might make the process of computation very inefficient. Therefore, in order to get a more efficient simulation, the variance reduction technique called importance sampling is used.

Prior to this Montecarlo optimization, another computational simplification is made. The whole uncertainty is translated to satellite 2, by adding the error ellipsoids, just the same way it was done in Patera's. This way, the dynamics of satellite 1 are completely known and, in satellite 2, the random generation of numbers is modified by adding up the value of the variances of the two satellites. With this computational shortcut, the time of calculation is almost halved.

The validity of this program enhancement is affirmed in the referenced paper[6] and finds its justification on the similarity of the orbits of the two satellites. Nevertheless, in order to confirm what is asserted in the mentioned document, some tests were performed comparing the

results obtained before and after performing the cited enhancement.

Now, in order to understand the need of importance sampling in the present problem, the following figures are presented.

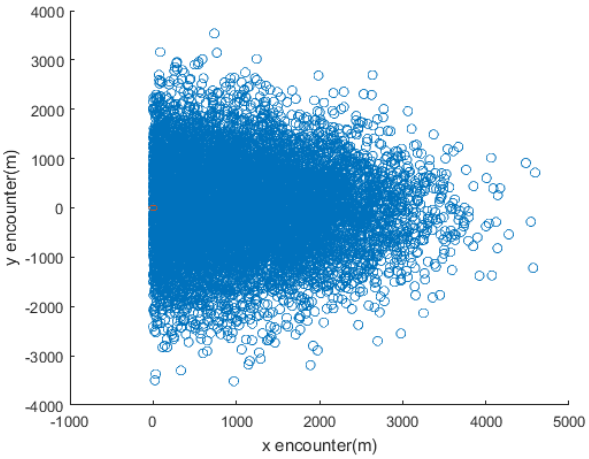

Figure 3.9: Crude Montecarlo inefficiency

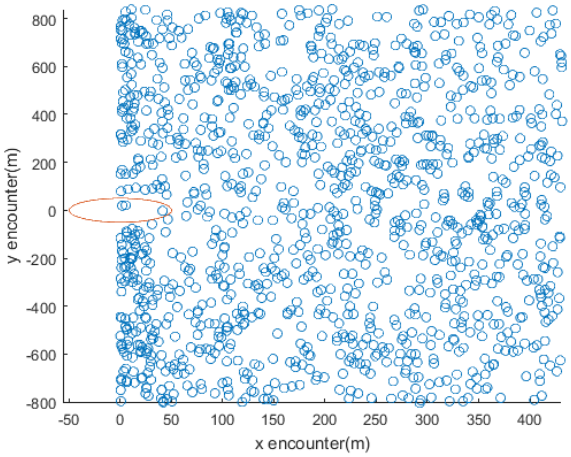

Figure 3.10: Crude Montecarlo inefficiency, zoom

They were obtained by plotting, for each run, the position of the satellite 2 with respect to satellite 1 at the point of closest approach and in the encounter frame, which is defined to be perpendicular to the velocity vector. It is visible that the majority of the points are very far from the hard body surface, depicted as a red circle; these points are giving not null information, but certainly very poor, in such a way that the variance of the results will not be acceptable until n is of the order of 10^6.

The technique to solve such a problem is called importance sampling. It consists of improving the initial random generation of points in such a way that one can concentrate each trial around the hard body radius. Evidently, by doing so, there is an alteration of the true distribution of the randomly generated initial positions, and as a result, a weighted correction for each trial is needed. Let us clarify this mathematically.
First of all, let us recall that our objective is to get the probability of collision:

$$p = \int H(x)f(x)dx = \mathbb{E}[H(X)] \tag{3.29}$$

which, in the case of Crude Monte Carlo, is given by estimated by equation 3.26.
Now, with importance sampling the integrand in equation 3.29 is multiplied and divided by the desired random distribution of points.

$$p = \int H(x).f(x).\frac{g(x)}{g(x)}dx = \int H(x).\frac{f(x)}{g(x)}.g(x)dx = \mathbb{E}\left[H(X)\frac{f(X)}{g(X)}\right] \tag{3.30}$$

Then, analogously to the Crude Montecarlo estimator, the importance sampling Montecarlo estimator is:

$$p = \frac{1}{n}\sum_{i=1}^{n} H(X_i)\frac{f(X_i)}{g(X_i)} \tag{3.31}$$

where $X_i \sim g(x)$. From the development of the expression of the new estimator, it is clear that this is unbiased whatever the distribution $g(x)$ may be. One only requires to choose a $g(x)$ such that whenever $g(x) = 0, H(x)f(x) = 0$ too, in order to avoid having singularities in the solution.

Nevertheless, if one chooses randomly the distribution $g(x)$, the target of importance sampling is unlikely to be achieve: not only one wants an unbiased estimator, but a certain estimator with a smaller variance, which depends basically on $g(X)$. Therefore, $g(X)$ must produce an initial state random generation near or inside the hardbody radius, as said before. In addition, as it is going to be proved below, $g(X)$ must be proportional to $H(X)f(X)$. This is clearly seen in the expression of the variance of the estimator, which is given by $Var_q = \sigma_g^2/n$:

$$\sigma_g^2 = \int \frac{((H(x)f(x)) - \mu g(x))^2}{g(x)} dx \tag{3.32}$$

where μ is estimated as $\mathbb{E}[H(X)]$.
Then, prior to build the distribution $g(x)$, there is the need to run a crude Montecarlo simulation to obtain the distribution $H(x)f(x)$. This is done not with the same number of runs than the ones required to get the right probability with Montecarlo, but with orders of magnitudes less runs. Otherwise, the method of importance sampling would be useless. And why can we perform less runs of Montecarlo to get $H(x)f(x)$? Because the shape of the distribution can be already appreciated with few runs simulations.

As an example of what has been said, for the case of $\Delta V = 0.3$, with a simulation of 10^5 runs, the plots showing $H(x)f(x)$ are depicted.

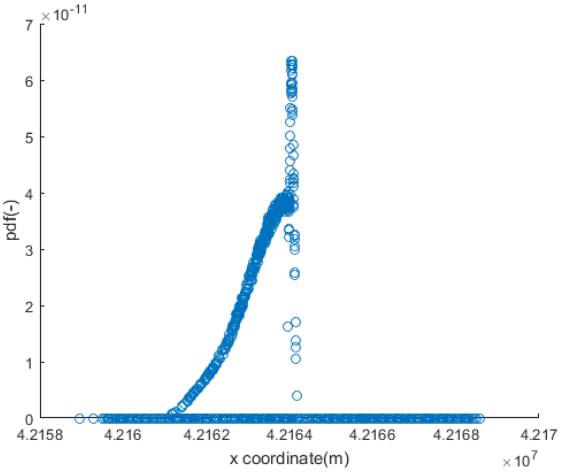

Figure 3.11: $H(x)f(x)$,x-axis

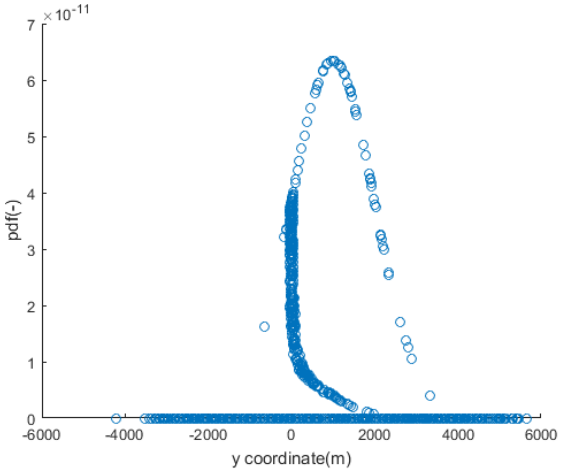

Figure 3.12: $H(x)f(x)$, y-axis

The scattered plots corresponding to the x and y axis are not attractive for us from the point of view of importance sampling. At a first sight, it seems that the variance of $H(x)f(x)$ is roughly the same of $f(x)$ (although it is true that in the case of x-axis, the resulting variance is half the original, because the 'bell' is cut on the middle). If this occurs, then $g(x)$ will be the same as $f(x)$ and importance sampling would be useless. However, in the case of z-axis, there is a great change on the variance of the distribution. The resulting probability distribution is dramatically squeezed. Undoubtedly, this is a good new for one wanting to implement importance sampling. When using this technique, applied to this particular problem, the PDF $g(x)$ will have a much smaller variance than $f(x)$.

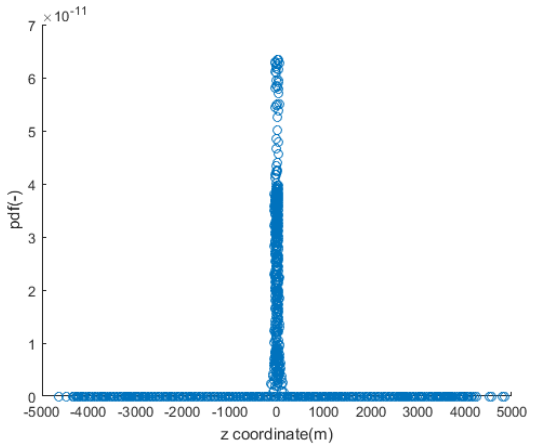

Figure 3.13: $H(x)f(x)$, z-axis

With the $g(x)$ as PDF for random initial position generation, the scattered position will now tend to concentrate around the hard body radius, making the efficiency of the Montecarlo simulation larger; this is, it reduces the variance.

So, let us see how the scattered points are distributed in the encounter plane when importance sampling is used, in contrast to what was obtained with Crude Montecarlo.

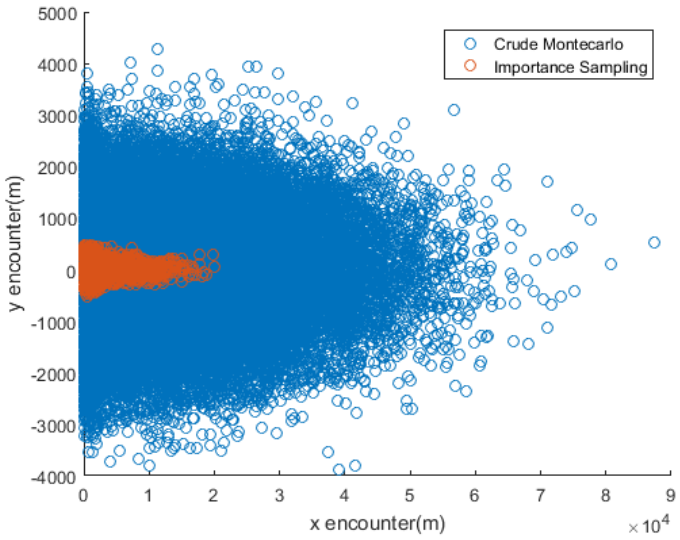

Figure 3.14: $H(x)f(x)$, z-axis

Clearly, the positions concentrate now nearer the hard-body, which is at the origin. Therefore, the output probability will converge faster for a given number of runs; as observed in the comparative histogram below, made with 10^4 runs per simulation.

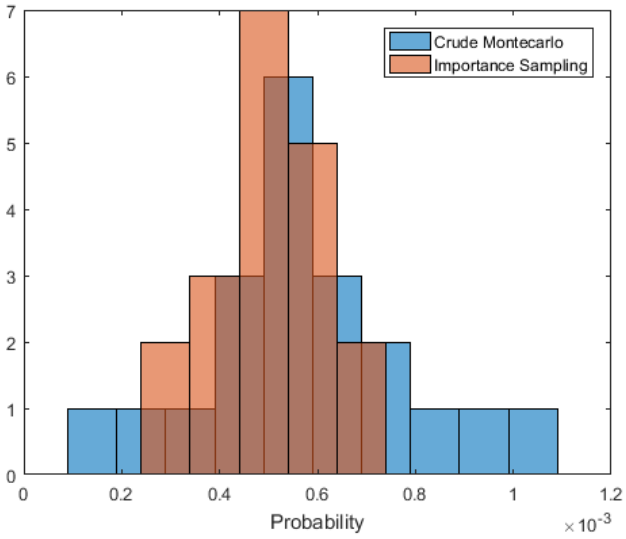

Figure 3.15: Crude Montecarlo vs. Importance Sampling

With 20 simulations per method, the histogram shows how the results of Importance Sampling concentrates around the solution more than those of Crude Montecarlo, which is the same as saying that the variance is reduced.

3.5 Introduction of the indexes for comparison

Prior to checking the validity of the method of Patera, let us define some indexes that numerically assess some characteristics of the relative motion between the satellite 1 and satellite 2. The goal is to understand whether or not these characteristics affect the accuracy of the method of Patera, as it was done in the referenced work [14]:

- **Linearity index**: it defines how much the velocity direction changes per unit of time. It tests the validity of assuming constant velocity direction along a single tube. Mathematically,

$$i_l = \frac{1}{\Delta t} arccos(\frac{\vec{v_a}\vec{v_b}}{|\vec{v_a}||\vec{v_b}|}) \tag{3.33}$$

  where $\vec{v_a}$ and $\vec{v_b}$ are two consecutive in time velocity vectors.

- **Thinness index**: it defines how different are the volumes of the gaps and overlaps of the tubes of the method of Patera.

$$i_t = \frac{r_{HB}}{d_M} \tag{3.34}$$

  where r_{HB} is the radius of the combined hardbody radius and Mahalanobis distance between the centers of the two satellites. Let us open now a brief parenthesis aiming at explaining what the Mahalanobis distance is and how it is defined in the case that concerns us.

  The Mahalanobis distance is a probabilistic concept which serves as a mean to measure how many standard deviations is a certain datum from the mean. It is a dimensionless distance, which would be equal to the Euclidean distance if the probability distribution

had as variance 1, in all directions. Particularizing the given definition for the present case, the resulting expression is the following:

$$d_M = \sqrt{(\vec{x}_2 - \vec{x}_1)^T \sum^{-1} (\vec{x}_2 - \vec{x}_1)} \tag{3.35}$$

where $\sum$ is the combined error covariance matrix. Notice that in the definition that we have just set, $(\vec{x}_2 - \vec{x}_1)$ does not represent the distance from the mean to a certain point, as it is exactly defined the Mahalanobis index, but the distance between satellite 1 and 2 at any instant. Thus, what is really measured in equation 3.35 is how many standard deviations there are between the two satellites. As a final point, in order to close the parenthesis, it is worth saying that, given that in the problems that are going to be solved in this work the error ellipsoid is assumed to be spheric in most of the cases, the equation 3.35 can be simplified to :

$$d_M = \sqrt{(d_x/\sigma_x)^2 + (d_y/\sigma_y)^2 + (d_z/\sigma_z)^2} \tag{3.36}$$

where $\{d_x, d_y, d_z\}$ are the coordinates of the relative distance between the two satellites.

- **Velocity index**: it defines how well the projection of the hardbody onto the encounter plane represents a sphere.

$$i_v = \frac{r_{HB}}{T|v|} \tag{3.37}$$

where T is the orbital period.

- **Dynamic index**: it measures how well the covariance can be kept constant over a time step.

$$i_d = \frac{1}{\Delta t} tr(P_a - P_b) \tag{3.38}$$

where P_a and P_b are two consecutive in time covariance matrices in the inertial reference frame.

Although this index is in general useful, it will not be so for the cases that will be analyzed in this work, because the error ellipsoids are assumed to be spherical and Patera's propagation does not consider any variation in the error distribution, thus P1 is always identical to P2.

As the reader may have already noticed, the indexes are defined to be calculated at each time step. Nevertheless, it is practical to have a single figure for a whole orbit in order to make comparison between different relative trajectories easily. For this reason, the L-infinity norm of the index for each orbit is taken as significant figure.

Chapter 4

Results

Let us now begin to deal with the analysis of the results obtained and the consequences which can derivate from the very analysis. It must be said that the first results that are to be displayed corresponds to the first case study, which will be analyzed with more detail than the others, since the conclusions that will be got out of it will be used to analyze the other two cases, which starts at section 4.2.

4.1 Comparing the results from different dynamic models

As pointed out in the beginning of the methodology section, it is necessary to determine what dynamic model is to be used in the calculation of probability. Certainly, without an analysis of the impact of the dynamic models on the estimation of the likelihood of a collision, the results obtained would be meaningless.

Clohessy-Wiltshire vs Kepler

Being conscious of the relevance of choosing the right model, Clohessy-Wilthsire and Kepler are analyzed and compared. Two different increments ΔV are analyzed, obtaining two type of plots: the first depicting the comparison between the relative trajectories of the two dynamic models, the second showing the absolute distance at any time between the satellites with both models.

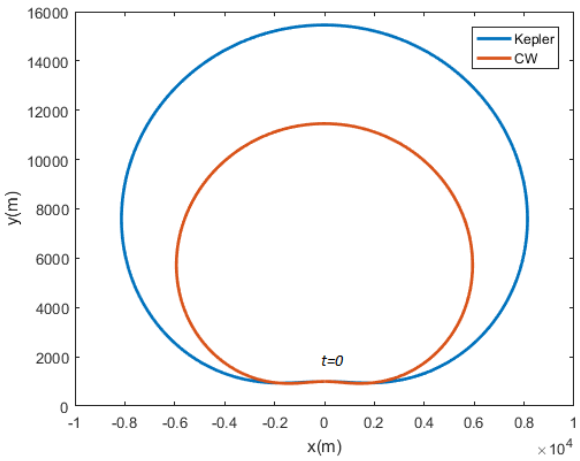

Figure 4.1: Relative position comparison, $\Delta V = 0.3$

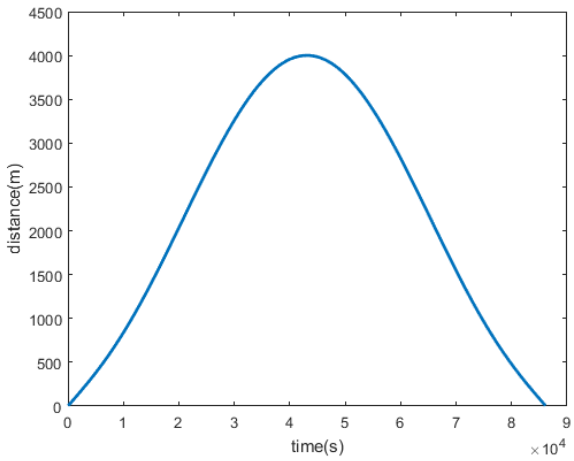

Figure 4.2: Difference between models, $\Delta V = 0.3$

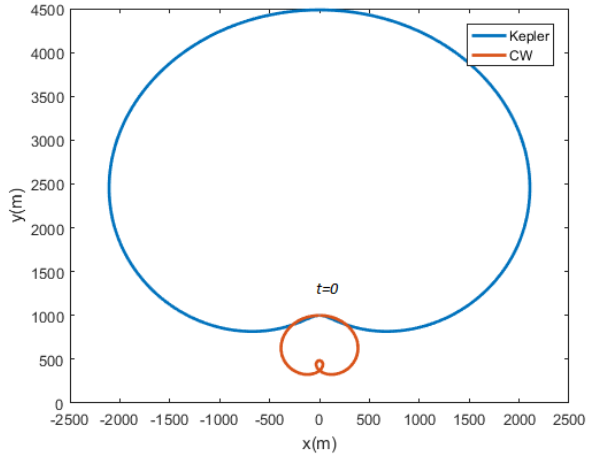

Figure 4.3: Relative position comparison, $\Delta V = 0.1$

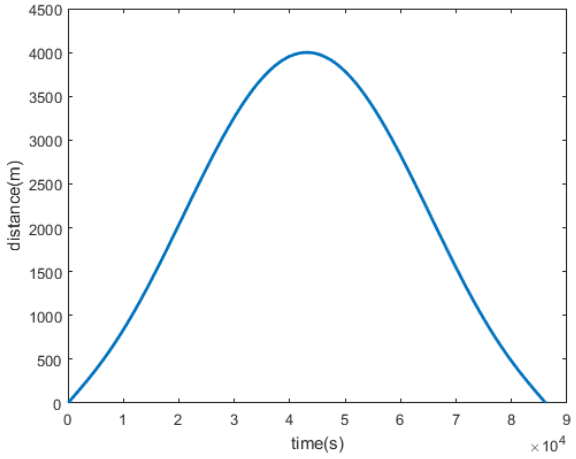

Figure 4.4: Difference between models, $\Delta V = 0.1$

The results obtained unveils the fact that the differences are large enough to affect importantly the calculations in a time span of one day. The order of magnitude of kilometers observed in the divergence between both trajectories, which is roughly constant for both cases, is not admissible for the calculation of probability in which the size of the hard-body is of 50 m and the standard deviation is 1 km. In order to confirm this assertion, the probability of collision is calculated with Patera's method using both dynamic models.

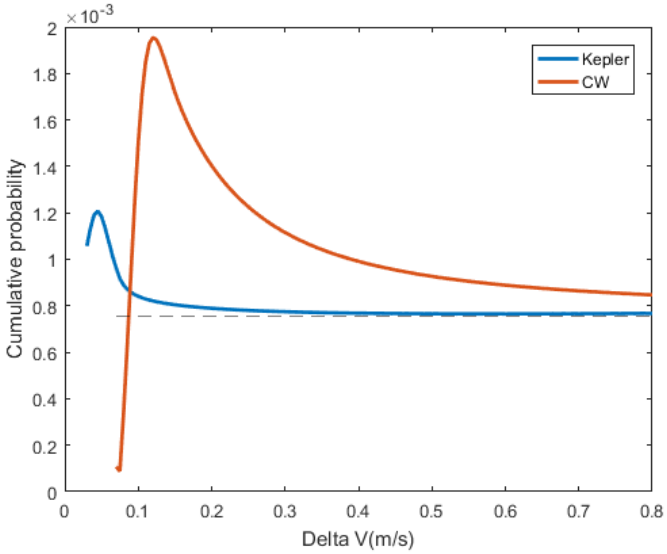

Figure 4.5: Probability of collision:comparison

As the Clohessy-Wiltshire approximation makes, for a given value of ΔV, the satellite 2 move closer to satellite 1 than in the Kepler model, then the probability curve obtained by Clohessy-Wiltshire is displaced towards the right. Moreover, due to the fact that for a given relative distance in both models, the relative velocities are different, the red curve is shifted upwards, since the probability of collision is proportional to the relative velocity(see equation 3.21). Therefore, although the computational time is smaller for the Clohessy-wiltshire approximation, one must use Kepler when calculating the collision probability for a time span of the order of one day.

One might end the comparison between the models by noticing the reduction of the discrepancy of the results when ΔV comes larger and larger. With the aim of explaining this observation, one must first note that as ΔV increases, so does the eccentricity of the orbit of the satellite 2. As a consequence, the dissimilarity between the trajectory of both orbits is larger and larger. Then, the encounters, when they take place, will be more and more shorter in time, and the satellites relative distance will be larger and larger, becoming the initial position of the satellites the moment of closest approach. Now, due to the shortness of the encounter, the probability calculation problem will be linear; and given what has been said before, it will have the point of closest approach where the propagation initiates. Therefore, the probability calculation will only depend on the points of the orbit around the initial position, where Clohessy-Wiltshire model is still good propagating the relative position. Here is why the solutions converge for large values of the increment of speed.

4.2 Validity of Patera's Method

Having Kepler as propagator of the state vector of both satellites, the comparison of the results obtained through Patera and Montecarlo is plotted here below, for the first case study.

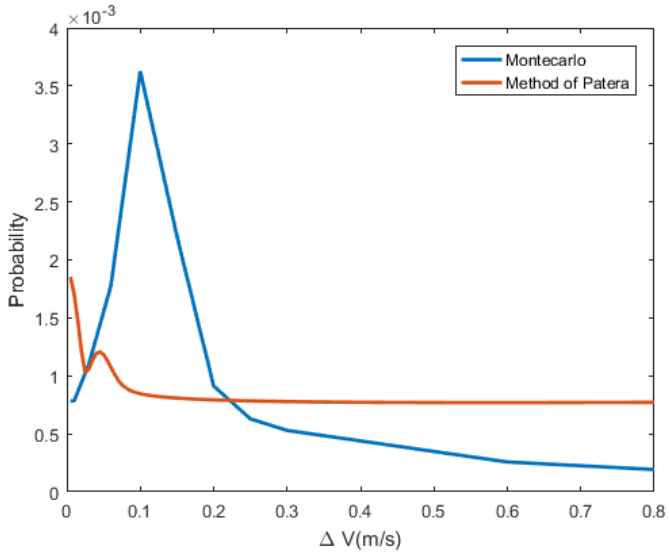

Figure 4.6: Patera vs Montecarlo

What is observed at first sight is that there exists a great discrepancy in the results for a certain interval of ΔV. The interval at which this occurs is small with values between 0.1m/s and 0.2m/s. The expression "great discrepancy " refers to the fact that the probability tool of Patera differs from the reference results of Montecarlo in more than 10^{-3} probability over 1, when the value taken as limit for the realization of a collision avoidance maneouver has been defined as 10^{-4}. Such a result will inevitably lead to the definition of a poor confidence interval for the method of Patera, which might result in a waste of fuel to perform unnecessary maneuvers; or worse, it might underestimate the collision probability, putting into risk the satellites integrity.

Yet, it should be noted that for larger values of ΔV, the method of Patera seems to get closer to the real solution. Comparing these results to those found in the literature, it is observed that similar orders of magnitudes of the error of the method of Patera are obtained in the referenced paper [14], in which the author analyzes Patera's tool for different types of orbit

geometries, but not specifically in the GEO case.

In order to understand the physics behind these results, let us plot now the evolution of the indexes previously defined with the increase in ΔV.

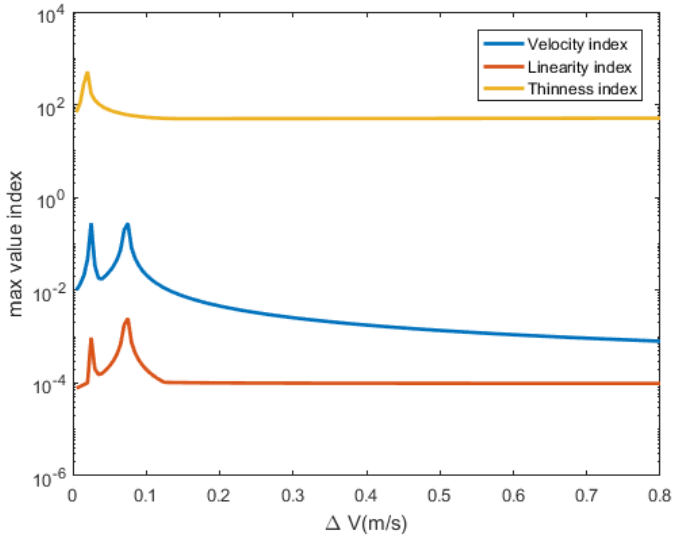

Figure 4.7: Indexes in logarithmic scale

What is observed is that the indexes are, in general, not very sensitive to the increase in the relative trajectory eccentricity. Nevertheless, there exists an increment of all the values for smaller ΔV, just when the error in Patera is greater. Certainly, the result is what was expected, since the indexes are defined in such a way that the lower they are, the better is the approximation of Patera: if the linearity index is small, then the velocity changes less and less from time step to time step;or if the thinness index is smaller, the probability associated to the gaps approaches that of the overlaps.

If one analyses deeply the linearity index (3.33), it will come up soon that no matter the curvature of the orbit, the method of Patera can adapt to such a parameter. If the index becomes too large, meaning that the curvature of the orbit is very pronounced, one just needs to reduce the time step to approach to the solution. Therefore, with an anlysis of the convergence of the results varying the time step length it would be enough to cope with this problem.

Regarding the thinness index (3.34), if its value is large, one can proceed by applying the easy solution that Patera proposes [13] or simply by reducing again the time step, in order to reduce the gaps and overlaps.

Certainly, the indexes provide useful information, but they seem to be useless to analyse what it is guessed to be the most important factor for analysing the error of the method of Patera: the propagation of the error ellipsoid. It could be undoubtedly argued that the indexes can tell us about how the error ellipsoid changes, but *a priori* it is not known which is such relation, if any. So let us proceed to analyze the evolution of the error ellipsoid and its influence on the calculation of probability.

Error ellipsoid propagation

In the method of Patera, the propagation of the error ellipsoid is made simply by keeping it constant in the local axis of the satellite. Intuitively, one will think this is not the correct way of propagating the ellipsoid, since the initial position uncertainty does not only affect the very initial position of the satellite, but all the orbital elements, which will determine the future trajectory of the satellite. Therefore, some changes on the position error ellipsoid are expected to occur which will be undoubtedly affecting the calculation of probability. In order to obtain the real state of the error ellipsoid at different times, and analyze how this changes from t_0 (at which the measurements are taken) to a given time t, the method of Montecarlo is used.
For this purpose, two plots showing the evolution of the variance(for a given ΔV) in the moving reference frame(at which the covariance matrix keeps diagonal) of the satellite are presented below(notice that in the x-axis the time is represented with the number of the time step, in such a way that 800 corresponds to the end of the propagation, 1 day; and 400 corresponds to half a day).

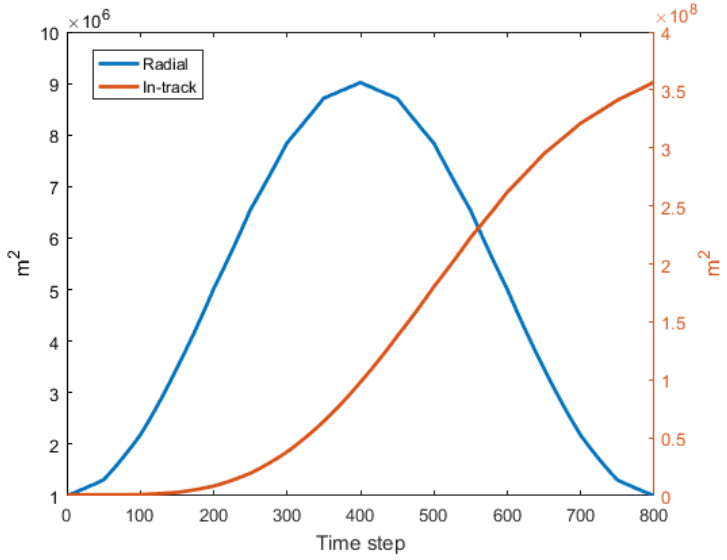

Figure 4.8: Evolution of the variance radial and in-track

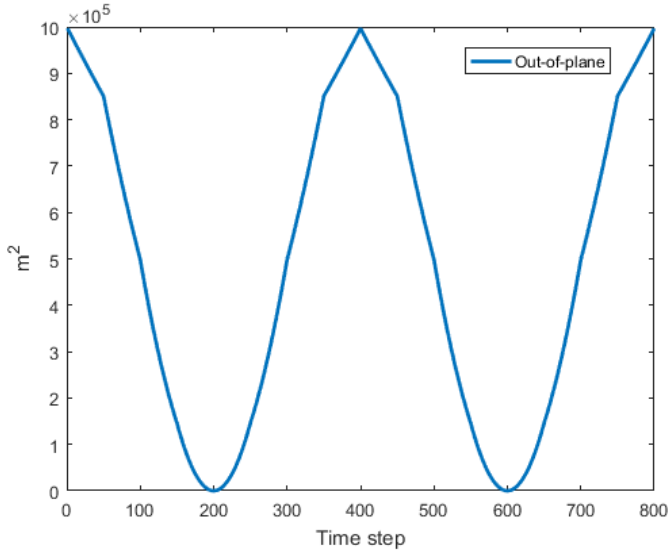

Figure 4.9: Evolution of the variance out-of-plane

The results depicted in the pictures confirm our previous assertion, which stated the variation of the error ellipsoid variance as it is propagated through time. The way in which the error ellipsoid varies is observed to be non-monotonic in two of its principal axes: it inflates and then it deflates. However, the in-track variation does not experiment a change on its growing trend. This result is also in agreement with what is found in literature. In addition, one should not forget to highlight the conclusion that rises from the fact that the covariance is diagonal in the moving reference frame: the error ellipsoid really rotates with the satellite on its orbital translation.

Evidently, these changes in the ellipsoid are a source of disagreement between Montecarlo results and Patera's methods results, given that Patera does not consider any change in the variance. This lack of consideration for the ellipsoid variation in Patera's method presumably affect significantly the calculation of the probability, something which will be studied later. In order to visualize better the error ellipsoid propagation, two plots are shown with its projection in two different planes (for the case of $\Delta V = 0.1$): the "mean" encounter plane (defined to be the encounter plane of the mean relative trajectory at the same time instant for which the Montecarlo propagation is frozen) and a plane perpendicular to it and to the plane of the relative orbit. These two 2D pictures permits us visualize the 3D shape better than a messy 3D representation.

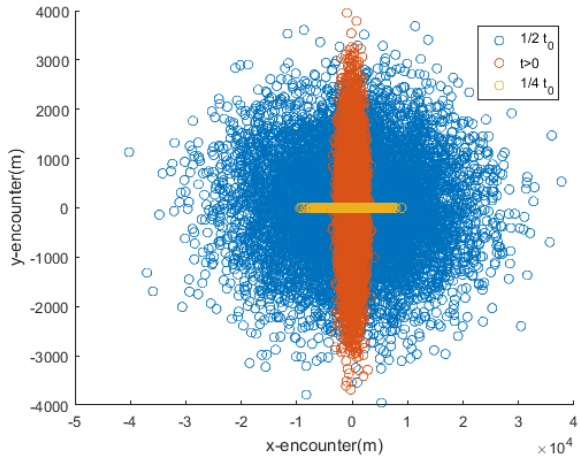

Figure 4.10: Ellipsoid in encounter frame, $\Delta V = 0.1$

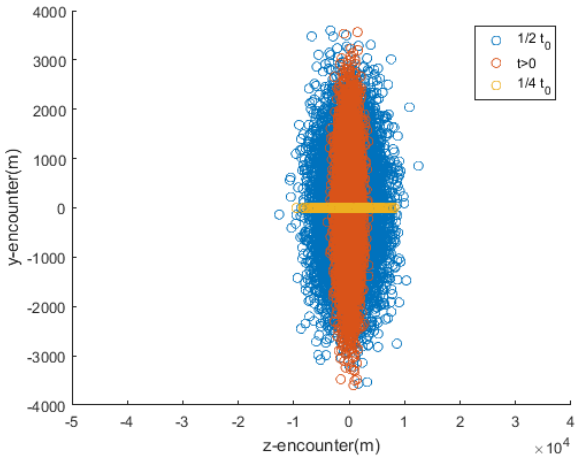

Figure 4.11: Ellipsoid in encounter frame, $\Delta V = 0.1$

Along the out-of-plane direction (which were named as y-axis in the encounter frame), when $t = 1/4t_{orbit}$ the standard deviation squeezes dramatically(see also figure 4.9), reaching a minimum to subsequently increase up to normal levels observed at $t = 1/2t_{orbit}$. This, *a priori*, singularity is explained by observing that the different trajectories, no matter their initial position elevation angle, crosses the equatorial plane at around the time instant $t = 1/4t_{orbit}$, as seen in the schematic figure 4.12, where the blue arrows represent the direction of propagation of the three initial positions(the blue dots) .

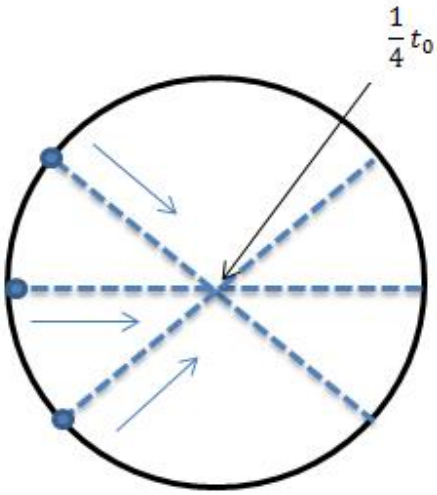

Figure 4.12: Convergence of orbits in $1/4t_{orbit}$

Let us not leave aside this question of the ellipsoid variation yet, since it could be interesting to study another point about it. It is the question of non-Gaussianities appearing in the orbital propagation.

What one finds in the literature is that there is an agreement that eventually in orbit propagation, non-Gaussianities become important enough so as to have a considerable impact on the final ellipsoid probability distribution. However, it is difficult to set a point at which one can say this occurs because of several reasons; such as the many different type of orbits to be analyzed, or the diversity of purposes for which propagation of covariances is made, which will differ in what can be considered as important impact on results of non-Gaussianities. The question of whether or not the probability density function remains Gaussian or not in the problem under study is also of the interest of this work, given its potential application in the last section of this work. Having made this comment, let us make a brief analysis on this topic. With this aim, the tables 4.2 and 4.3 are displayed. They contain, for different $n\sigma$ values, the probability of finding a point inside the interval$(n\sigma, -n\sigma)$ in any of the three axes(of the moving reference frame). It should be pointed that σ is found for each of the three axes, by using the Matlab function $fitdist$, and setting the Gaussian PDF as the one to fit the probability. Then, knowing this, one may expect that if the points distribution is really Gaussian, at each time step the error ellipsoid must fulfill the *68 95 99.7 99.9 rule*. This is:

Probability	1σ	2σ	3σ	4σ
Initial density	0.6872	0.9545	0.9973	0.9999

Table 4.1: 3D Gaussian probability distribution

Thus, what is found, for two different ΔV, after one complete orbital period is the following:

Probability	1σ	2σ	3σ	4σ
Radial	0.6829	0.9547	0.9973	0.9999
In-track	0.6824	0.9549	0.9972	0.9999
Out-of-plane	0.6849	0.9548	0.9975	0.9999

Table 4.2: $\Delta v = 0.1m/s$

As observed, the distributions in the three axes keep roughly Gaussian, with a slight variation of lower order of magnitude than the probability. Evidently, depending on the application, one should consider if this is Gaussian enough or not. For the topic that concerns us, this issue will be analyzed in the section of *Alternative method*.

Probability	1σ	2σ	3σ	4σ
Radial	0.6810	0.9538	0.9973	1.000
In-track	0.6812	0.9543	0.9971	1.000
Out-of-plane	0.6827	0.9545	0.9974	1.000

Table 4.3: $\Delta v = 0.3m/s$

Once the error ellipsoid evolution is known, it is possible to analyze the influence it has in the calculation of the probability of collision. Below, the plot of the contribution to the total probability of each time step in the method of Patera, in the time of one orbital period, is shown, for two different ΔV. As it can be seen, the parts that contributes the most to the total probability are near the beginning and the end of the period, which means that the point of closest approach is near the initial position of the satellite.

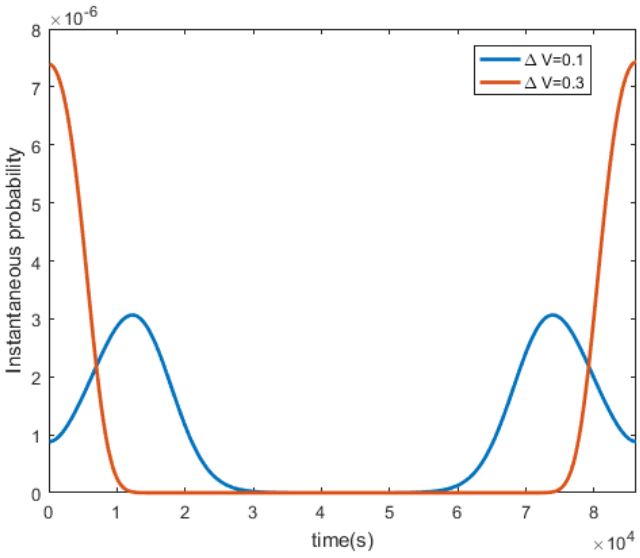

Figure 4.13: Instataneous probability, Patera

Nevertheless, the most interesting fact concerning the study of error covariances is the perfect symmetry that exists with respect to the point corresponding to half of the orbital period. Indeed, this symmetry tells us that the error covariance has kept constant throughout the whole motion with the present method. Why? Because the symmetry that exists in the relative dynamics can only result in a symmetric instantaneous probability distribution if the covariance matrix is constant, or if its behavior during the motion is also "symmetric". Evidently, it is known that is constant because this is what we set in the method of Patera.

Then, if this is what it is observed with a constant error ellipsoid, one would expect an asymmetric probability distribution in the real case, where the error covariance changes asymmetrically along the motion. Certainly, this is what occurs.

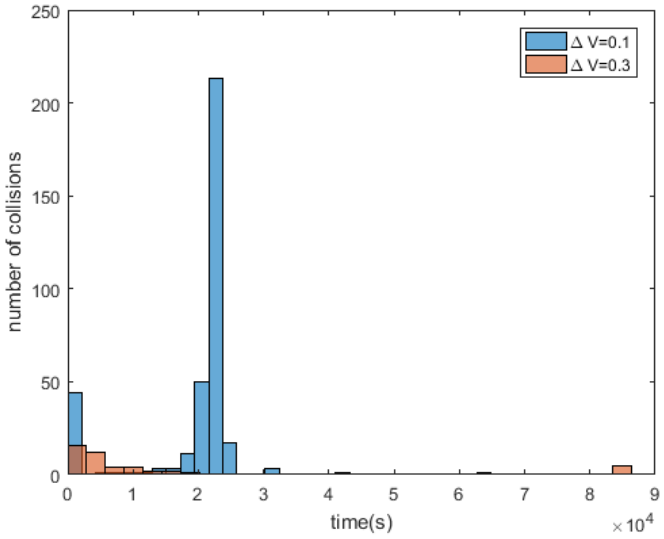

Figure 4.14: Histogram: number of collisions along the orbital time

In the histogram which is above these lines, the evolution of the "real" instantaneous probability is depicted for the two same cases that were analyzed before. The histogram represents the number of collisions that are registered by the method of Montecarlo, and at which time interval they occurred for each run out of the 10^5 that were taken to make this plot.

As it was deduced, the asymmetry is notable, meaning a great discrepancy with what Patera method yields. Clearly, the major contribution to the total probability of collision is coming from the first half of the orbital period.

Let us try to explain now what can be the connection between the difference in the instantaneous probability distribution in Patera and Montecarlo, and the evolution of the error ellipsoid. As observed in figures 4.8 and 4.9, the evolution of the in-track variance is of monotonic and fast growth, resulting in a final covariance matrix of a much larger size than the initial one (even though the other two diagonal terms of the covariance matrix may behave symmetrically). Then, the dispersion of the propagated positions near the end of the orbital period provokes that the probability of having a collision between the two satellites reduces. Here is the reason for the change in instantaneous probability distribution along the orbital period.

A further analysis is worth doing on the comparison of figures 4.13 and 4.14, because with them it is finally demonstrated that the error ellipsoid propagation is the major source of error of the method of Patera. In order to close the argumentation, we retrieve the plot with which this section was opened (Figure 4.6). If one takes the $\Delta V = 0.3$ m/s in the mentioned figure, what is observed is that the probability of collision output from Patera's method is larger than that obtained from Montecarlo. What was unclear after an analysis of the indexes that had been defined, becomes now evident as one sees how the dilution of the error ellipsoid reduces to almost 0 the contribution to the total probability of the time interval near one orbital period. It is even more interesting to analyze the other case: with $\Delta V = 0.1$ m/s. This time, the probability obtained by means of Montecarlo method is larger than the one obtained by Patera's. Although this may sound contradictory, if one only attends to what has been said about the dilution of the error ellipsoid, it is indeed coherent if one observes the huge increase in the

instataneous probability at 1/4 the orbital period in the method of Montecarlo with respect to Patera. Again, the reason for this behaviour is found in the error ellipsoid variation. For $\Delta V = 0.1$ m/s, unlike in the case of 0.3 m/s, the point of closest approach of the satellites (with most significant contribution to the total probability) is at 1/4 the orbital time. At this time instant, as we have already seen in this section, the out-of-plane variance reduces dramatically. This creates a concentration of points in the orbital plane, which cannot result but in a large increase of the collisions between the satellites, which imply a not less large increase in the probability of collision obtained with Montecarlo.

Therefore, as a last step in the analysis of the results, the way in which the error ellipsoid varies during the satellite translation directly links the dynamics to the error observed in Patera: depending on the interval of time during which the satellites are closer, the error ellipsoid will have a shape (and size) or another, and so, the error of the method of Patera will be one or another, depending almost uniquely on the error ellipsoid shape and size.

Up to this point, only the results of one possible encounter scenario has been displayed. Therefore, in order to demonstrate that the conclusions already obtained can be extrapolated to other GEO satellites relative trajectory, it is proceeded to analyse the other two case studies defined in the methodology section.

Second case study

In order to proceed in the same way it was doing in the previous case, let us plot the relative dynamics of the satellites for different ΔV, as seen from the non-inertial reference frame attached to satellite 1.

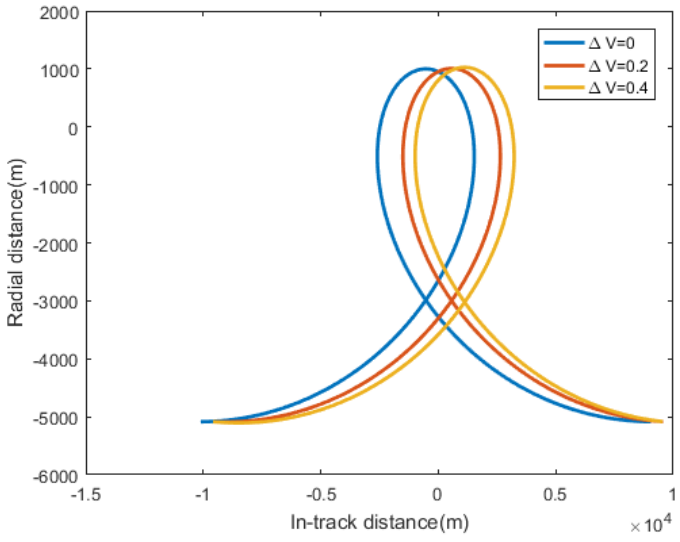

Figure 4.15: Trajectories in rotating reference frame

It might be worth remembering firstly that dynamics are keplerian, as demonstrated to be required in case of propagation of time spans of the order of 1 day. What is concerning the characteristics of the relative trajectory, it must be noted that as the increment on speed applied at $t = 0$ increases, the relative distance at the point of closest approach reduces. In principle, this could make us assert that the probability would increase with ΔV. However, that certitude would only exist in case that the encounter were a short time encounter, as seen

in section 2.3. But this is not the case since the encounter happens during a relatively "long time", while the trajectory encircles the origin of coordinates; and all those points encircling the origin may some important impact on the probability. What has been said aims at deepening into the meaning of short and long-term encounter; it does not mean that the probability is not going to grow monotonically, it just means that it does not have to.

Having made this point about the dynamics, what follows is to introduce the comparison between the output probability of the method of Patera and the one of Montecarlo.

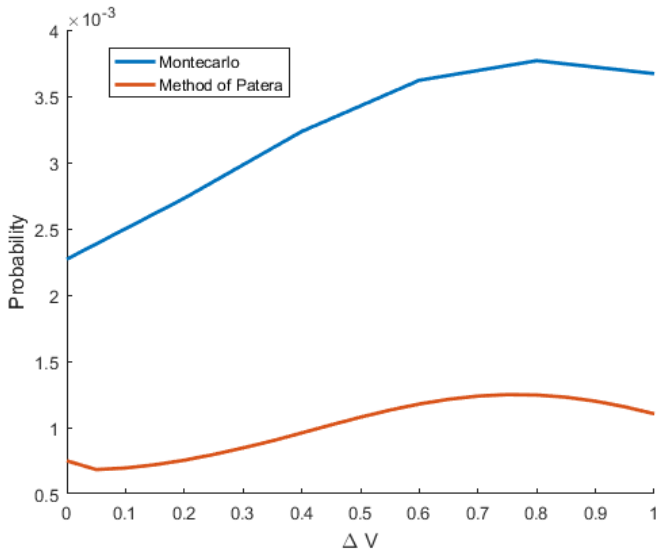

Figure 4.16: Trajectories in rotating reference frame

Again, as it occurred with the results in the previous case, Patera's method differs with Montecarlo's outputs by an order of magnitude of 10^{-3}. On the other hand, unlike what was found in the preceding situation, the differences between both methods seem not to change significantly with ΔV: there is nearly a vertical shift between results. Such a difference might be related to the fact that the time interval at which the satellites are closest is roughly the same for all the trajectories simulated. So, the direct link, which was shown in the previous case, between dynamics and error of Patera's method holds, yielding the already mentioned vertical "shift".

Keeping the analogous way of proceeding, the contribution to the total probability of collision from the different orbital times is found.

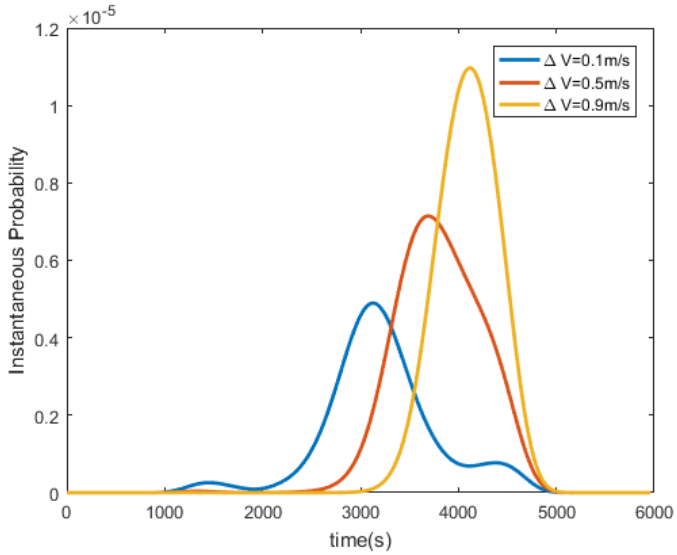

Figure 4.17: Instantaneous probability of collision

This time, in general, there does not exist any symmetry in the output of Patera's method, as a result of the assymetry of the dynamics.Yet, in particular, for the case of $\Delta V = 0.1$ m/s, given that the dynamics are closed to being symmetric with respect to 1/2 the period of the orbit, the probability distribution is closed to symmetry.

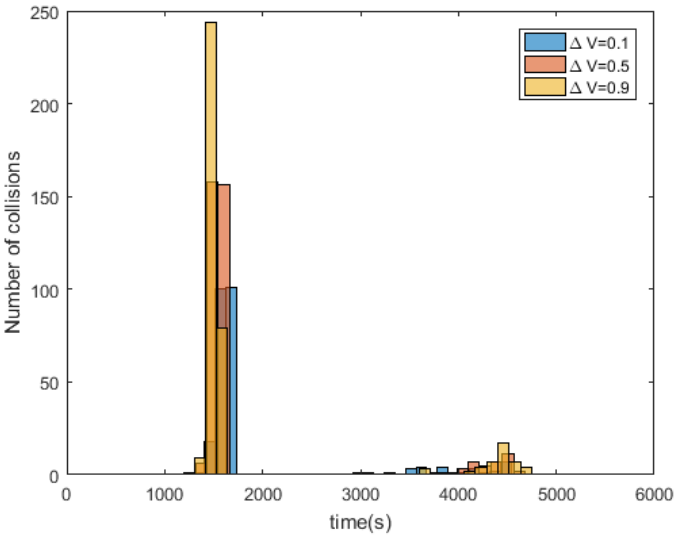

Figure 4.18: Number of collision along the orbital time

In the same fashion to what was seen for a $\Delta V = 0.1$ m/s in the previous case study, the dramatic reduction of the variance in the out-of-plane direction (the plot of the variance is not shown, because is pretty similar to figures 4.8 and 4.9), combined with an slight approach of the satellites (as seen in the zoom of figure 4.17, below these lines), near the time 1/4 the orbital period makes that the main contribution to the total probability, obtained by means of Montecarlo, comes from that time interval. The contribution for 3/4 the orbital period is not as important given that, although the out-of-plane variance is also very much reduced, the variance in the in-plane directions has increased significantly, and the probability of collision dilutes.

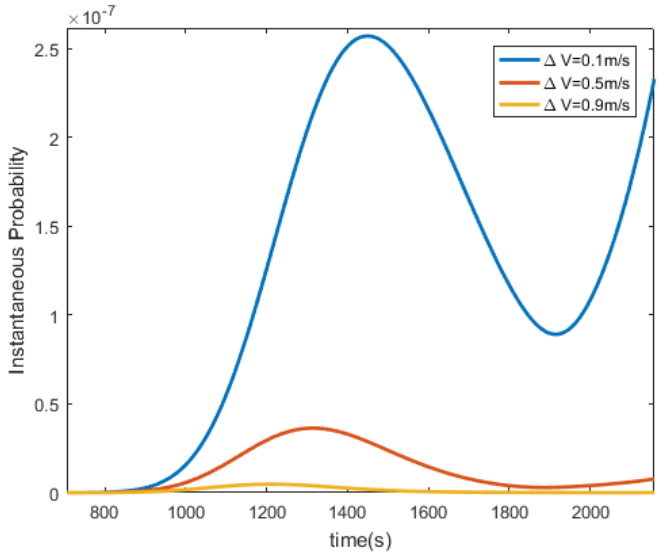

Figure 4.19: Instantaneous probability of collision, zoom at 1/4 orbital period

Third study case

The last of the three cases, as said in the methodology section, will permit us understand the way in which Montecarlo behaves in the analysis of a collision avoidance maneouver in GEO.

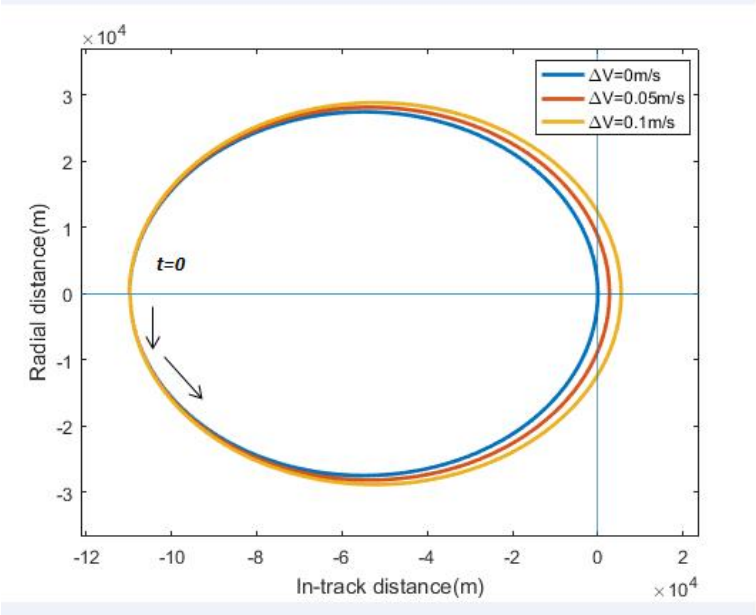

Figure 4.20: Relative dynamics, third case study

The evolution of the trajectories with ΔV is shown in Figure 4.20. What is shown in the plot is coherent with what was said in the definition of the third case study; this is, that in case of no thrust impulse at $t = 0$, both satellites eventually(at $t = 1/2$ the orbital time) come as close as being just at the same position. Therefore, one expects that the probability of collision will be maximum if no action is taken, while it will be decreased as the thrust impulse becomes larger. In addition to this, this case is worth being studied because it has the particularity, which is not found in the previous cases, that the main contribution to the probability of collision

concentrates at 1/2 the orbital time. At least, that is what the relative trajectories geometry seem to indicate.

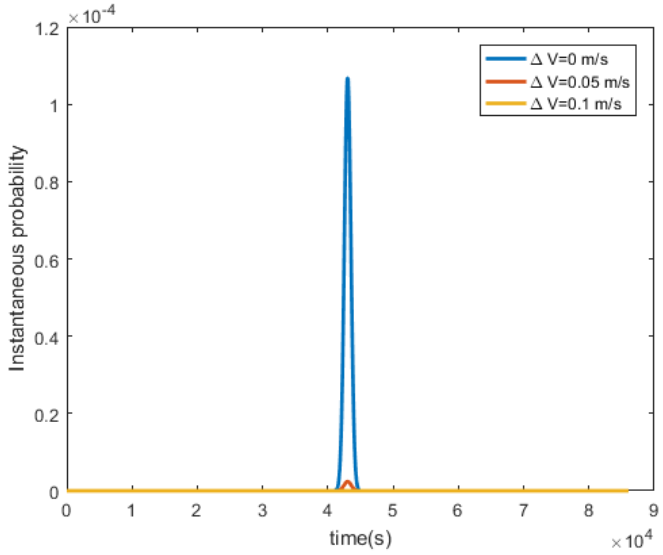

Figure 4.21: Instantaneous probability,Method of Patera

The figure 4.21 confirms our guess. Now, the effect of the probability of collision contribution concentrating at 1/2 the orbital period can be deduced by applying what has been learned so far about the evolution of the error ellipsoid in GEO. According to figures 4.8 and 4.9, extrapolating the results, at half the orbital period, the error ellipsoid out-of-plane term should be keeping roughly the initial value, while the other two terms should have experienced an important increase; thus, as the variance should get larger, the probability of collision would diminish.

The preceding reasoning is coherent with what figure 4.22 displays. The method of Patera, in which the error ellipsoid keeps constant while propagating the nominal trajectory, outputs a larger value than that obtained through Montecarlo, at which there is the mentioned dilution of the probability.

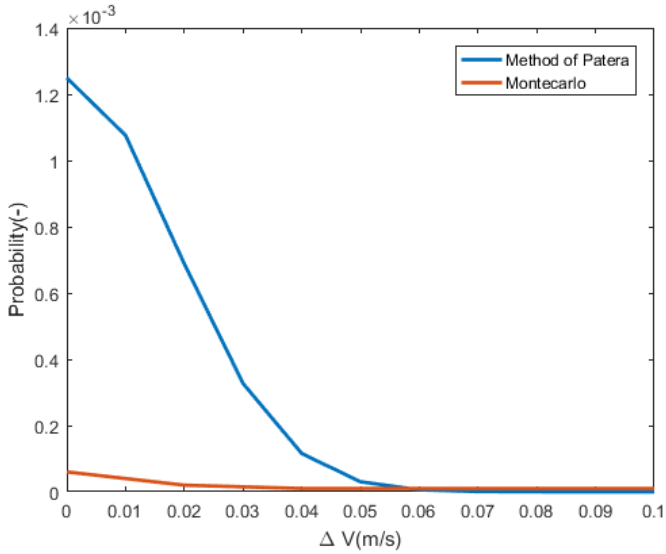

Figure 4.22: Patera vs Monteacarlo, third case study

Obviously, the divergence between the methods is smaller as ΔV increases, this is, as the minimum distance between the satellites increases and the probability of collision reduces. Both methods tend to 0 with the increment of the velocity at $t = 0$, and so, their disagreement decreases.

After having analyzed this last case, one crucial point must be made. This is about the convenience of making use of Patera's method as indicator of the probability of collision. Notice that in this last case, the output of Patera is conservative with respect to the "real" value, while in the other cases this does not happen. Evidently, in all the cases a considerable disagreement is observed between the two outputs, but it is far more attractive to have an overestimation of the probability than having an underestimation, due to the consequences that would derive from each of the two scenarios.

Therefore, after having seen that the inflation of the error ellipsoid (the increase of the variance) is what makes the estimation of Patera conservative, and knowing that the variance continuously grows due to the in-track term (the other two varies sinusoidally, figures 4.8 and 4.9); one can conclude that the method of Patera will be better for estimating probability of collisions for satellites which get closed to each other beyond 1/2 the orbital period when the error ellipsoid has inflated. Against this restriction of the scope of the method of Patera, one can argue that in the first case study, the probability of collision estimation was also conservative when ΔV was larger than around 0.3, which the reader might remember to be when the encounter occurred near $t = 0$. Certainly, this is right, but it will be, in general, of no interest to calculate the probability of collision when the moment of closest approach will take place very few time after the estimation is made.

Difference in computational time

Up to this moment, the difference in computational time between Patera and Montecarlo has only been mentioned qualitatively, not quantitatively. It is due then to show what is the great advantage of the studied method against Montecarlo.

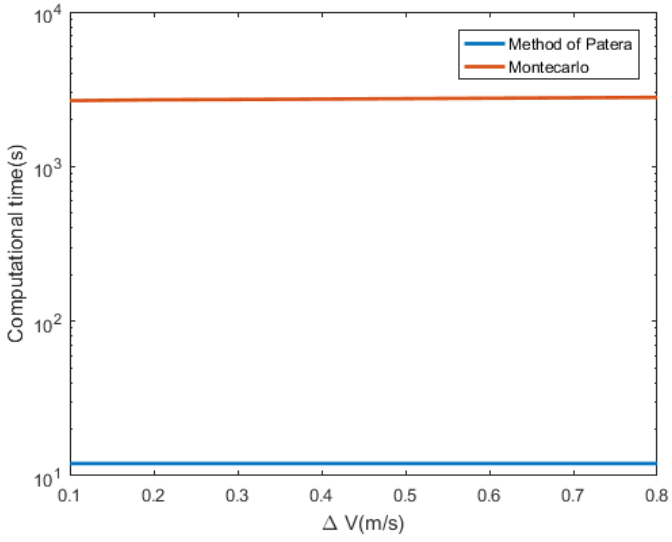

Figure 4.23: Difference in computational time, first case study

The plot is obtained for the first case study and it unveils that the method of Patera is orders of magnitudes less expensive(in terms of computational cost) than Montecarlo. The results for the other two cases are similar, and so, the plots are not plotted here.

Having this in mind, it is up to the user to decide whether or not the saving of computational time can compensate the magnitude of the error which have been shown up during this work for long term encounters, particularly to encounters in GEO.

Chapter 5

Alternative Method

In view of the results and the analysis made of the previous section, an improving of the method of Patera is proposed so that the results obtained fit better the "real" probability, the one obtained by means of Montecarlo.

As discussed in the lines that precede this section, the issue of covariance propagation is seen as the most important source of error in Patera's method; many things have been said thereon. Therefore, the method that is about to be proposed must enhance, in some way, the way the method tackles the problem of propagation. It has been seen in the introduction that there exist numerous techniques that aim at propagating the covariance matrix efficiently, without propagating with Montecarlo. These methods are, in general complex, although certainly useful. Opposed to this complexity, it is proposed here a simple method which consists of a combination of Montecarlo and Patera. Let us firstly describe the method; later, once the methodology is clear, it should be easier to explain why it could imply an enhancement of the method of Pater; and finally, the results obtained will be evaluated.

Methodology

The first step in the method is to propagate the nominal trajectory with the a certain dynamic model (in the present case, Kepler is used). Then, the dynamic states obtained are inputted to a Montecarlo simulation. The nominal trajectory is used to measure the deviation of the different trajectories simulated with respect to the nominal. This way, the error ellipsoid can be obtianed at different points in the satellite trajectory as:

$$E_e(t) \equiv \{\vec{x}_{mean}(t) + \Delta\vec{x}(t), \overline{\overline{C'}}(t)\} \tag{5.1}$$

where $\overline{\overline{C'}}(t)$ is the covariance matrix obtained by Montecarlo simulation at an instant t, and $\Delta\vec{x}(t)$ the error in the mean with respect to the nominal trajectory. In addition, a correction for the velocity is also obtained.

This tracking of the error ellipsoid is done with a certain time step which is fixed by the user, and which is not the same as the one required to assure precision in the solution of the pure Montecarlo method(see section 3.4) In fact, the time step is expected to be much larger, so that the number of points at which the error ellipsoid is measured is significantly reduced, with respect to pure Montecarlo. The reason for this will be given in the next section.

The updated error covariances, the mean deviation as well as the velocity correction, which are output of the simulation of Montecarlo, will input subsequently Patera's probability tool,

together with the nominal trajectory obtained previously. Then, the method of Patera is implemented but updating the error ellipsoid each time step previously defined. In addition, at the orbital points among the ones at which the updating is done, the uncertainty in the position is obtained by linear interpolation of the standard deviation, as follows:

$$\sigma^2(t) = \left(\sigma_1 + \frac{\sigma_{i+1} - \sigma_1}{t_{i+1} - t_i}(t - t_i)\right)^2 \tag{5.2}$$

where σ^2 are the entries of the diagonal covariance matrix. For the position mean and the velocity, the procedure is analogous.

Now, as a consequence of what has been shown in previous sections , that the principal axes of the ellipsoid rotate with the satellite translation, one should be careful to perform the interpolation not in the inertial frame of reference, but in the moving reference frame (with radial and in-track axes). This is what is depicted schematically in figure 5.1.

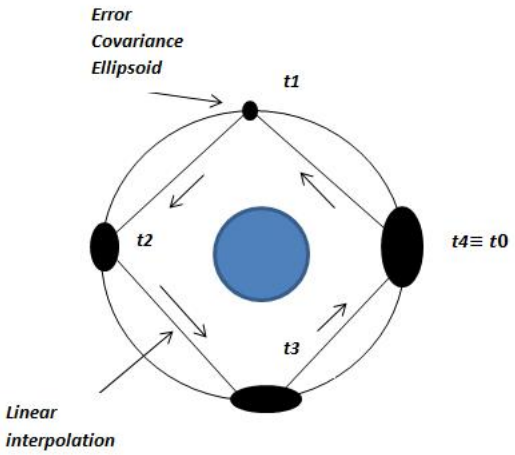

Figure 5.1: Schematic view of the ellipsoid updating

In order to make the reader better understand the method, the flow chart of picture 5.2 was built.

Foundations of the method

Until now, the proposed method could be thought to be useless since, in the end, it is needed to perform the well-known costly Montecarlo simulation. Wasn't that what we were trying to avoid with the creation of new methodologies, to avoid Montecarlo simulation? The answer is yes... and no at the same time.

Yes, since certainly the method of Montecarlo is really time-consuming and computationally inefficient.

Nevertheless, *no* as well. The reason is that if one is able to reduce enough the number of simulations to be run as well as the number of time steps in the propagation, the computation time of Montecarlo can be drastically decreased. Indeed, this is what the proposed method does by combining Patera's tool with Montecarlo.

This reduction of the computational time of Montecarlo is achieved thanks to the two facts that follow:

- Firstly, the error ellipsoid diagonal terms in the moving reference frame attached to the satellite are well approximated through linear interpolation with a small number of error ellipsoid state recording. Such a characteristic which can be observed in figures 4.8 and 4.9, permits reducing the number of time steps in the Montecarlo simulation.
- Although Montecarlo may require 10^6 or even 10^7 runs to get an accurate result, for getting the input error ellipsoid for Patera it is enough with at least 10^4 runs. The reason for this to occur is the different way in which Patera and Montecarlo calculates probability. The latter is very sensitive to small changes in the probability distribution: a small divergence might mean having a 0, instead of 1, or vice versa. Conversely, the method of Patera varies slightly with small changes in the probability distribution because the probability of collision is obtained through an integral.

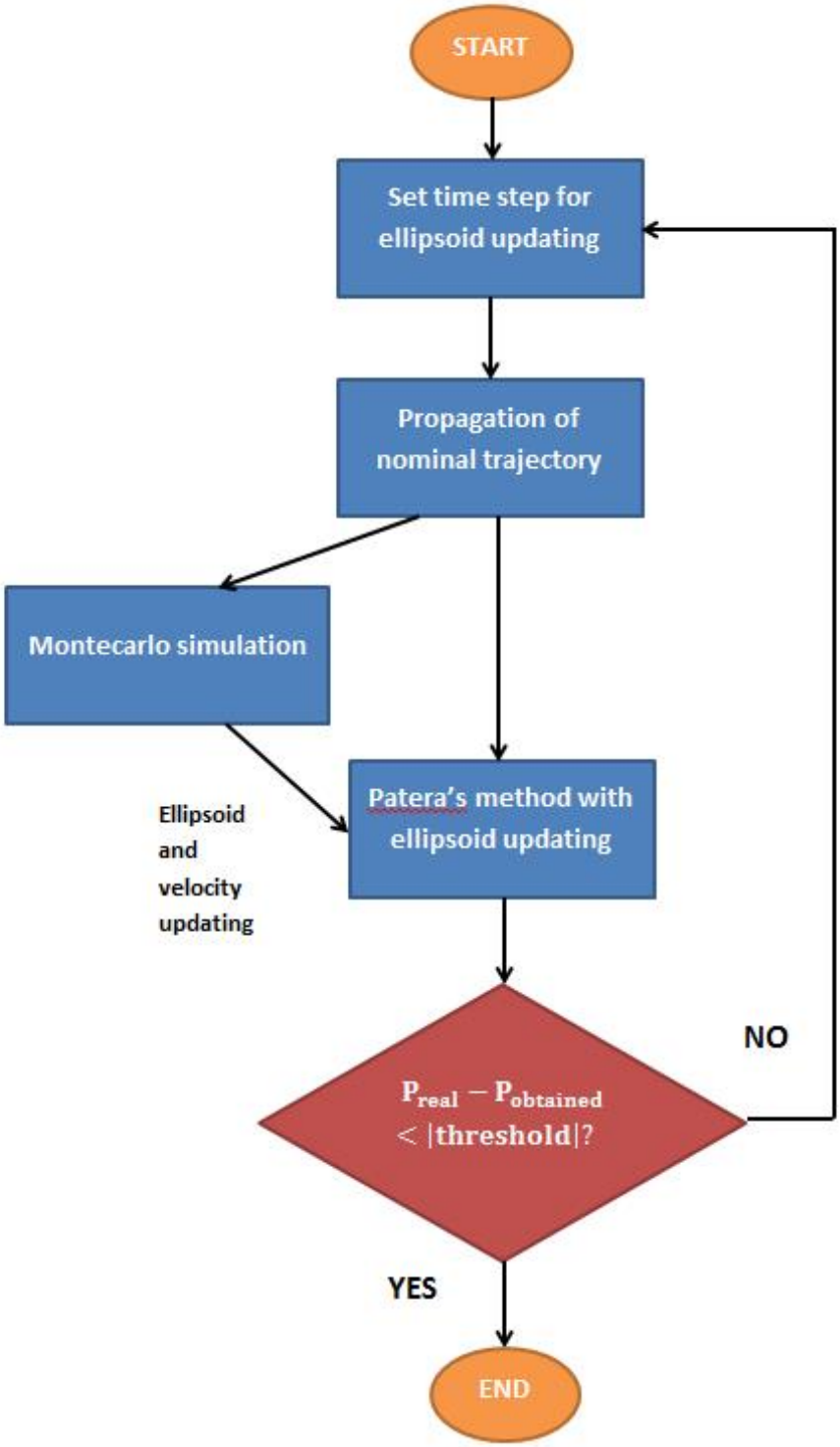

Figure 5.2: Flow chart

Results and conclusions

Knowing the methodology as well as the foundations on which the method rests, it is now possible to evaluate what is the method's value (if any) through the analysis of the results, being the ones below these lines corresponding to the first case study, compared to the results of Montecarlo.

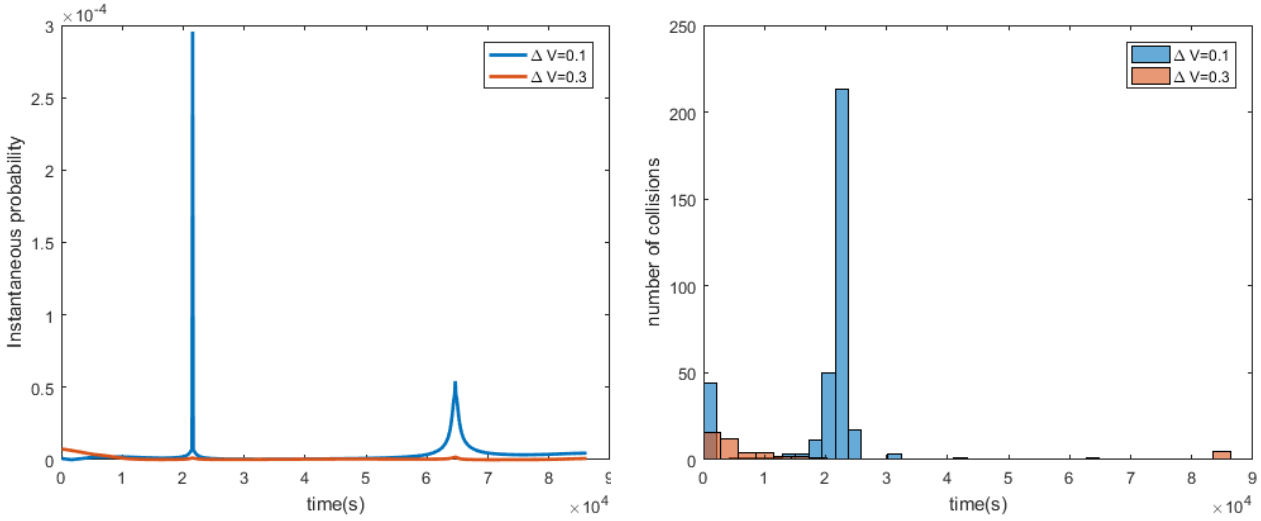

Figure 5.3: New method vs Montecarlo, instantaneous collision probability

They were obtained for two different values of ΔV and, as said during the methodology, reducing to 10^4 the number of runs in Montecarlo, as well as the number of time steps in the propagation.

What the graphs unveil is that the new method achieves to approximate well the distribution of the instantaneous probability, as it is outputted from Montecarlo. Indeed, the symmetry that was observed in figure 4.13 for Patera's method's results is now broken and the instantaneous probability of collision concentrates at the first half of the orbit period.

Nevertheless, in spite of this remarkable fact of the "true" instantaneous probability distribution being matched by the new method, there is a problem concerning inputting into Patera the velocity correction: having run the method several times with a fixed $\Delta V(= 0.1)$, what is observed is a great dispersion on the results:

	Target	1^{st} run	2^{nd}run	3^{rd}run	4^{th} run	5^{th} run
Probability	**0.0036**	0.0028	0.0079	0.0023	0.0064	0.0026

Table 5.1: Variation of the new method's output

which is known to be caused by the velocity correction input; since if only the position mean and covariance updating is inputted into Patera, a great convergence in the results is observed. This is what unveils figure 5.4, in which convergence is achieved(obviously, with a wrong result, since the velocity correction is not inputted) by performing a Montecarlo simulation with only 16 time steps for a time span of 1 day(this is, 16 mean and covariance updatings), and only 10^4 runnings. In such a way that the computational time of Montecarlo turns from around 2 hours into less than ten seconds.

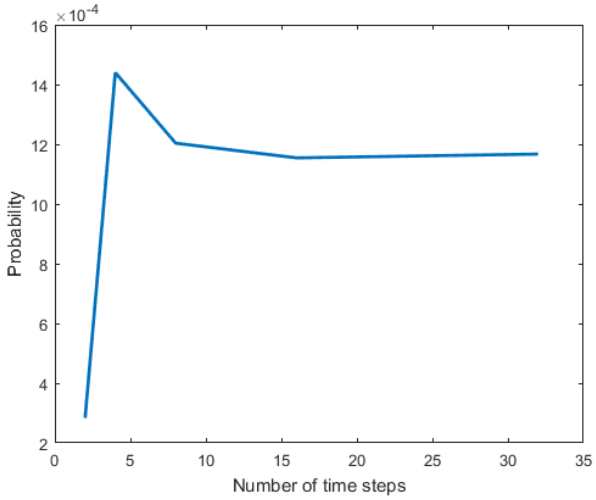

Figure 5.4: Convergence with the number of time steps for updating, with a Montecarlo simulation of 10^4 runnings

As it has been shown, although small errors in the mean and variance of the position do not affect significantly the probability calculation(which is the foundation of the method); this does not hold when it comes to velocity errors.
The root cause of this poor performance of the method might lay on the fact that, together with the correction on the velocity, it should be inputted as well the velocity uncertainty. This, although initially is considered to be zero, does not remain null throughout the propagation. On the contrary, it increases with the position error. Unfortunately, the method of Patera is not designed to input velocity uncertainty, and it is out of the scope of this work to investigate that, although it might be interesting as a future work project.

Chapter 6

Conclusion

Along the present work, the method of Patera for calculating the probability of colision in GEO orbit was tested. With that goal, the reference values to which compare the results were those obtained by means of Montecarlo simulation, improved with Importance Sampling to reduce its variance. Out of this analysis, it was concluded that for a time span of one orbital period, Patera's method diverges from the "real" probability with values of the order of magnitude of 10^{-3}, when the upper limit had been set as 10^{-4}. Nevertheless, it was shown that Patera's tool could be of interest to analyze cases at which the encounters are likely to occur after a time larger than 1/2 the orbital period. This is due to the fact that the estimations, although far from the real value, were demonstrated to be conservative in those cases.

In addition to that, aiming at solving the error of Patera's method, which was found to be the propagation of the error ellipsoid, a new method was proposed consisting on updating the state of the error ellipsoids with inputs of Montecarlo. Nevertheless, the method failed due to the lack of consideration of the velocity error uncertainty of the method of Patera. So, finding a way of inputting the velocity uncertainty in the probability tool could be an interesting line of research.

Finally, it is worth saying that prior to the analysis mentioned in the lines above, the dynamic model of Kepler was proven to be the propagator needed for probability calculations of at least one day of time span. Clohessy-Wiltshire is not enough accurate for such a purpose.

Bibliography

[1] Salvatore Alfano. A numerical implementation of spherical object collision probability. *Journal of the Astronautical Sciences*, 53(1):103, 2005.

[2] Salvatore Alfano. Addressing nonlinear relative motion for spacecraft collision probability. In *AIAA/AAS Astrodynamics Specialist Conference and Exhibit*, page 6760, 2006.

[3] F Kenneth Chan. *Spacecraft collision probability*. Aerospace Press El Segundo, CA, 2008.

[4] Ken Chan. Analytical expressions for computing spacecraft collision probabilities. In *Proceedings of the 11 th Annual AAS/AIAA Space Flight Mechanics Meeting, Santa Barbara, CA*, pages 305–320, 2001.

[5] Inter-Agency Space Debris Coordination Committee et al. Iadc space debris mitigation guidelines. *URL: http://www. iadc-online. org/Documents/Docu/IADC_ Mitigation_ Guidelines_ Rev1_ Sep07. pdf [c ited: 20 July 2011]*, 2007.

[6] JC Dolado, P Legendre, R Garmier, B Revelin, and X Pena. Satellite collision probability computation for long term encounters. *Adv. Astronaut. Sci*, 142, 2011.

[7] Ya-zhong Luo and Zhen Yang. A review of uncertainty propagation in orbital mechanics. *Progress in Aerospace Sciences*, 2016.

[8] Kyoko Makino and Martin Berz. Remainder differential algebras and their applications. *Computational differentiation: techniques, applications and tools*, pages 63–74, 1996.

[9] David McKinley. Development of a nonlinear probability of collision tool for the earth observing system. In *AIAA/AAS Astrodynamics Specialist Conference and Exhibit*, page 6295, 2006.

[10] Noelia Sánchez Ortiz. Methodologies for collision risk computation = metodologías para cálculo de riesgo de colisión. 2015.

[11] Russell P Patera. General method for calculating satellite collision probability. *Journal of Guidance, Control, and Dynamics*, 24(4):716–722, 2001.

[12] Russell P Patera. Satellite collision probability for nonlinear relative motion. *Journal of Guidance, Control, and Dynamics*, 26(5):728–733, 2003.

[13] Russell P Patera. Collision probability for larger bodies having nonlinear relative motion. *Journal of guidance, control, and dynamics*, 29(6):1468–1472, 2006.

[14] Michael R Phillips. Spacecraft collision probability estimation for rendezvous and proximity operations. 2012.